



## Streamflow response to seasonal snow cover mass changes over large Siberian watersheds

Daqing Yang,<sup>1</sup> Yuanyuan Zhao,<sup>1</sup> Richard Armstrong,<sup>2</sup> David Robinson,<sup>3</sup> and Mary-Jo Brodzik<sup>2</sup>

Received 4 April 2006; revised 18 August 2006; accepted 18 December 2006; published 11 May 2007.

[1] We used remotely sensed weekly snow water equivalent (SWE) data (1988–2000) to investigate streamflow response to seasonal snow cover change in the large Siberian watersheds (the Ob, Yenisei, and Lena basins). We quantified the seasonal cycles and variations of snow cover mass and river streamflow and identified a clear correspondence of river discharge to seasonal snow cover mass change. We also examined and compared the weekly mean streamflow with the weekly basin SWE for the study period. The results revealed a strong relation between the streamflow and snow cover mass change during the spring melt season over the large Siberian watersheds. This relationship provides a practical procedure of using remotely sensed snow cover information for snowmelt runoff estimation over the large northern watersheds. Analyses of extreme (high/low) SWE cases (years) and the associated streamflow conditions indicate an association of high (low) flood peak with high (low) maximum SWE in the Ob and Yenisei basins. Comparative analyses of weekly basin SWE data versus snow cover extent (SCE), peak snowmelt floods, and climatic variables (temperature and winter precipitation) indicate consistency among basin SWE, SCE, and temperature but incompatibility between basin SWE and winter precipitation, particularly for the Lena watershed. The inconsistency suggests uncertainties in determination of basin winter snowfall amounts and limitations in applications of the SWE retrieval algorithm over large watersheds/regions with very different physical characteristics. Overall, the results of this study clearly demonstrate that the weekly SWE data/products derived from microwave remote sensing technology are useful in understanding seasonal streamflow changes in the arctic regions.

**Citation:** Yang, D., Y. Zhao, R. Armstrong, D. Robinson, and M.-J. Brodzik (2007), Streamflow response to seasonal snow cover mass changes over large Siberian watersheds, *J. Geophys. Res.*, 112, F02S22, doi:10.1029/2006JF000518.

### 1. Introduction

[2] River discharge is a primary driver of the Arctic Ocean freshwater budget. The amount and variation of this freshwater inflow critically affect the salinity and sea ice formation, and may also exert significant control over global ocean circulation [Aagaard and Carmack, 1989]. Arctic hydrologic systems exhibit large temporal variability due to large-scale changes in atmospheric circulation [Proshutinsky *et al.*, 1999; Walsh, 2000; Semiletov *et al.*, 2000]. This variation significantly influences the cross-shelf movement of water, nutrients and sediments. Examination of streamflow changes in the major northern river basins and their relations to surface climate and atmosphere is

critical to better understand and quantify the atmosphere-land-ocean interactions in the Arctic and their consequent global impacts.

[3] Snow cover significantly affect atmosphere, hydrology, permafrost, and ecosystem in the high-latitude regions. Snow cover melt and associated floods are the most important hydrologic event of the year in the northern river basins [Kane, 1997; Kane *et al.*, 2000]. Recent investigations show that snowmelt has started earlier over the recent decades in the northern regions, such as Canada, Alaska, and Siberia, associated with warming in winter and spring seasons [Whitfield and Cannon, 2000; Brabets *et al.*, 2000; Serreze *et al.*, 2000; Zhang *et al.*, 2001; Lammers *et al.*, 2001; Yang *et al.*, 2002; Ye *et al.*, 2003]. Studies demonstrate that the timing and magnitude of northern river streamflow are strongly allied with cold season snow cover storage and subsequent melt [Rango, 1997; Cao *et al.*, 2002; Yang *et al.*, 2003]. Therefore the changes in snowmelt pattern may indicate a hydrologic regime shift over the high latitudes [Yang *et al.*, 2002; Serreze *et al.*, 2002]. Our current knowledge of large-scale snowmelt processes and their interaction with climatic change and variation is

<sup>1</sup>Water and Environmental Research Center, University of Alaska Fairbanks, Fairbanks, Alaska, USA.

<sup>2</sup>National Snow and Ice Data Center, University of Colorado, Boulder, Colorado, USA.

<sup>3</sup>Department of Geography, Rutgers University–State University of New Jersey, Piscataway, New Jersey, USA.

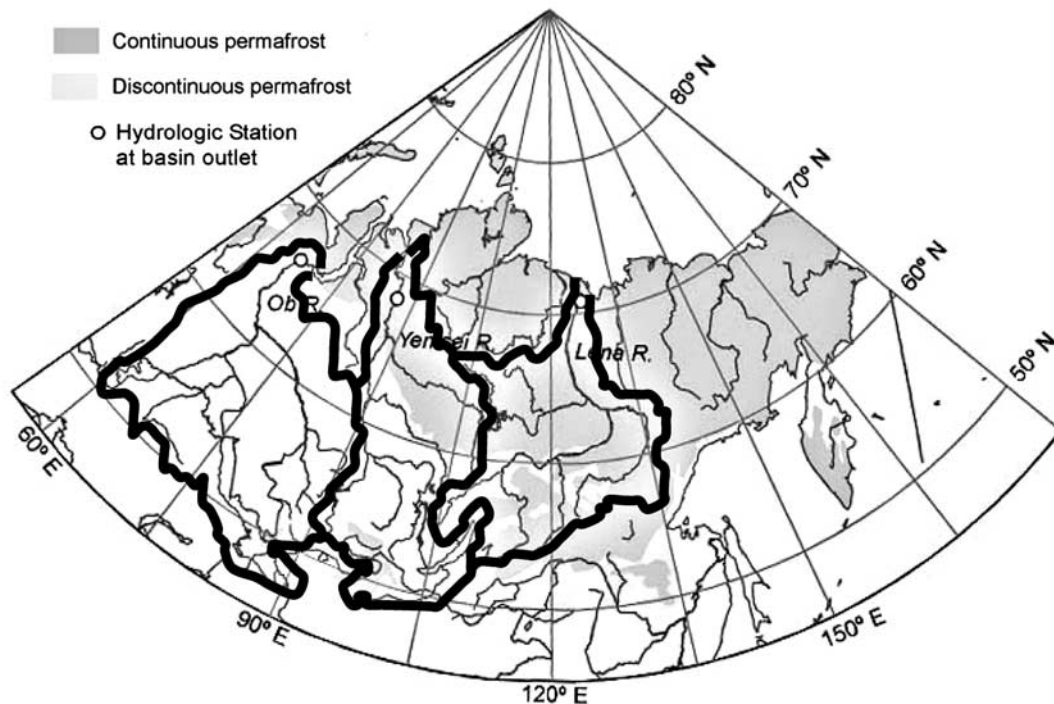


**Figure 1.** Three largest rivers (the Lena, Yenisei, and Ob) in Siberia. Also shown are permafrost distribution, basin boundaries, and hydrologic stations at the basin outlets.

incomplete, particularly for the arctic regions with insufficient ground-based observations [Vörösmarty *et al.*, 2001]. This limits our ability of understanding past changes and predicting future changes of the hydrology system under a warming climate in the high-latitude regions.

[4] Remotely sensed snow data have been very useful to cold region climate and hydrology investigations [Massom, 1995; Steffen *et al.*, 1993]. For instance, the NOAA weekly snow cover data set (maps) over the Northern Hemisphere permits quantitative assessments of changes and variations in regional snow extent [Robinson *et al.*, 1993; Robinson and Frei, 2000; Frei and Robinson, 1998, 1999; Serreze *et al.*, 1993; Clark *et al.*, 1997], and they are useful for hydrologic and snowmelt runoff models [Rango, 1996, 1997; Rango and Shalaby, 1999]. Yang *et al.* [2003] recently used the weekly NOAA snow cover extent (SCE) data to study streamflow hydrology in the large Siberian rivers. In addition, long-term snow water equivalent (SWE) data have been derived from the passive microwave sensors [Chang, 1997; Chang *et al.*, 1987; Armstrong and Brodzik, 2001, 2002]. Their potential value for large-scale hydrology and climate studies in the high-latitude regions has not been systemically evaluated. This study will assess the compatibility of the passive microwave SWE data over three large watersheds in Siberia, and examine the streamflow response to snow cover mass change particularly during the spring melt season. The objective is to determine the potential of using remotely sensed snow cover mass information to enhance our capability of snowmelt runoff modeling over the large northern river basins with continuous and discontinuous permafrost. Changes in seasonal snow cover conditions may have significantly contributed to the ground surface temperature increase. The influence of seasonal

snow cover on soil temperature, soil freezing and thawing processes, and permafrost has considerable impact on carbon exchange between the atmosphere and the ground and on the hydrological cycle in cold regions/cold seasons [Zhang, 2005]. The results of this study will improve our understanding of the impact of climate variation and change on cold region hydrologic processes.

## 2. Data Sets and Methods of Analyses

[5] The Lena, Yenisei and Ob rivers are the three largest rivers in the Arctic. Their combined discharge contributes more than 45% of total freshwater flow into the Arctic Ocean [Shiklomanov *et al.*, 2000; Prowse and Flegg, 2000; Grabs *et al.*, 2000]. These large, northern flowing watersheds stretch from mid latitudes to the arctic coast (Figure 1). Their drainage areas range from 2,400,000 to 3,000,000 km<sup>2</sup> and are mostly underlain by continuous and discontinuous permafrost [Brown and Haggerty, 1998; Zhang *et al.*, 1999]. Since the late 1930s, hydrological observations in the Siberian regions, such as discharge, stream water temperature, river ice thickness, and dates of river freezeup and breakup, have been carried out by the Russian Hydrometeorological Services, and the observational records are quality controlled and archived by the same agency [Shiklomanov *et al.*, 2000]. Some of these data are now available to this study for the period from 1930s to 1999. In this study, long-term daily discharge records collected at the basin outlet stations are used for analyses. Large dams and reservoirs were built in Siberia regions for power generation, flood control, and irrigation during mid-1950s to 1980s. Studies show that reservoirs regulation alters hydrologic regimes particularly in the regulated sub-basins [Yang *et al.*, 2004a, 2004b; Ye *et al.*, 2003]. Our

recent analyses of daily streamflow data over the large Siberian basins indicate similarity in reservoir operation and regulation among years. For instance, the downstream peak streamflow over the regulated Lena basin always occurs in the spring snowmelt season, and its fluctuation between years is similar to the unregulated upper subbasins. This consistency in streamflow regime and variation allows us to use the observed data to explore streamflow-snow cover relation over the large basins.

[6] Maps of snow extent and snow water equivalent (SWE) derived from passive microwave satellite data (SMMR and SSM/I) for the Northern Hemisphere have been produced at the NSIDC [Armstrong and Brodzik, 2001, 2002] using a modified version of the Chang *et al.* [1987] algorithm. Regional maps and products have also been developed in Canada from the SMMR and SSM/I data, and used for analyses of snow cover variations over space and time [Walker and Goodison, 1993; Derksen *et al.*, 2000; Walker and Silis, 2002]. Although the algorithm used in this study [e.g., Armstrong and Brodzik, 2002] is not able to consistently detect wet snow, only nighttime or early morning (“cold”) orbits are used here, reducing the chance that wet snow is present. A subset of the NSIDC data representing the Arctic watersheds for the period 1988–2001 is used in this study to examine the seasonal and interannual variations of snow cover. Oelke *et al.* [2003] applied these SWE data for the active layer depth modeling in the Arctic. In addition, the NOAA weekly snow cover maps based on visible data are quite reliable at many times and in many regions including the high latitudes. They have been widely used for hydrologic and climatic analyses in the cold regions, such as development of basin snow cover depletion curves [Rango, 1996, 1997; Skaugen, 1999], study of streamflow response to snow cover changes in large northern rivers [Yang *et al.*, 2003], input snow cover data to regional hydrologic and snowmelt runoff models [Rango, 1997], and validation of climate model performance [Yang *et al.*, 1999; Frei and Robinson, 1999].

[7] The daily NSIDC Northern Hemisphere SWE data (EASE-grid) [Brodzik and Knowles, 2002] have been used in this study to generate weekly basin mean snow water equivalent (SWE) time series for the large Siberian rivers during 1988–2001. On the basis of these weekly records, we examine the seasonal changes of snow cover mass, by defining the SWE climatology based on weekly statistics, determining the dates of snow cover formation/disappearance and duration of snow cover/snow-free days, and quantifying the rates of snow cover mass change during the accumulation and melt seasons. We also derive weekly discharge time series from the daily streamflow data collected at basin outlets, and use the weekly data to describe the seasonal streamflow changes, including discharge regime, rates of streamflow rise and peak flow during the melt period. We calculate the weekly correlation of streamflow with basin SWE, and determine the consistency between SWE and streamflow changes over the seasons. Furthermore, we identify extreme SWE cases and examine their correspondence with river discharge conditions. These analyses define the weekly relationship between snowmelt runoff and basin SWE changes for the large watersheds in Siberia. In addition to streamflow and snow cover data, basin mean weekly precipitation and temperature time series during

1966–1998 have been created based on gridded global data sets [Jones, 1994; Hulme, 1991], and used to investigate the compatibility of SWE data with climate variables and to explain the streamflow response to seasonal snow cover changes.

### 3. Weekly Snow Water Equivalent

[8] The seasonal cycle of snow water equivalent from microwave satellite data over the Siberian regions is presented in Figure 2. The annual SWE regime includes week 53 due to leap years. It shows that both the accumulation and ablation processes are different among the large watersheds mainly due to temperature and precipitation differences between the western and eastern Siberian regions. Snow cover begins to form around late September (weeks 38–40) in Siberia. During the accumulation period, the Ob basin mean temperatures are warmer by 4.5°C in September and 7.8°C for October, respectively, relative to the Lena watershed (Figure 3a). Similar amounts of precipitation (about 45 mm) fall in both basins in September (Figure 3b). The cooler temperatures during late September over the Lena basin lead to the early formation of snow cover over the eastern Siberia. Snow accumulation rates generally are higher in the eastern regions and lower in both central and western Siberia. The highest accumulations occur during late November to early December in Siberia, i.e., about 11.3 mm/week in the Lena basin, 7.6 mm/week over the Yenisei watershed, and 8.2 mm/week for the Ob catchment. Snow cover reaches the maximum accumulation in mid February, with the peak SWE being about 120 mm (week 7) in the Lena basin, 80mm (week 7) in the Yenisei watershed, and 85 mm (week 8) in the Ob River. Snow cover mass decreases very slightly during weeks 8–11 perhaps due to sublimation and occasionally weak melt in the upper (south) parts of the basins (Figure 2).

[9] Snowmelt season starts over Siberia around mid-March (week 12–13). In the Ob basin snow cover depletion rate is very high during late March to mid April (weeks 13–16), SWE was reduced by 65% within 3 weeks. The Lena basin snow cover melts rapidly during mid April to mid May (weeks 16–19), while the Yenisei river snowmelt rate generally is slower, reducing only 50% SWE in more than 6 weeks (Figure 2). The strongest melt was 20mm during week 15 in the Ob basin, 10mm in week 14 over the Yenisei basin, and 17mm during week 18 in the Lena basin. Snow cover disappears around early June in Siberia, i.e., week 23 in the Ob basin, week 26 in the Yenisei watershed, and week 24 in the Lena basin. The snowmelt periods vary from 17 weeks in the Ob basin, 16 weeks in the Yenisei watershed, to 14 weeks in the Lena catchment (Figure 2). The shorter melt season suggests a faster melt of the thicker snow cover over eastern Siberian regions due to late onset of melt associated with higher temperatures during late spring. To illustrate snowmelt processes over Siberia, Figure 4 presents an example of weekly SWE changes over a typical melt season (week 13–24) in 1991.

### 4. Compatibility of Basin SWE Data

[10] Temperature and precipitation are the main factors affecting snow cover characteristics including accumulation

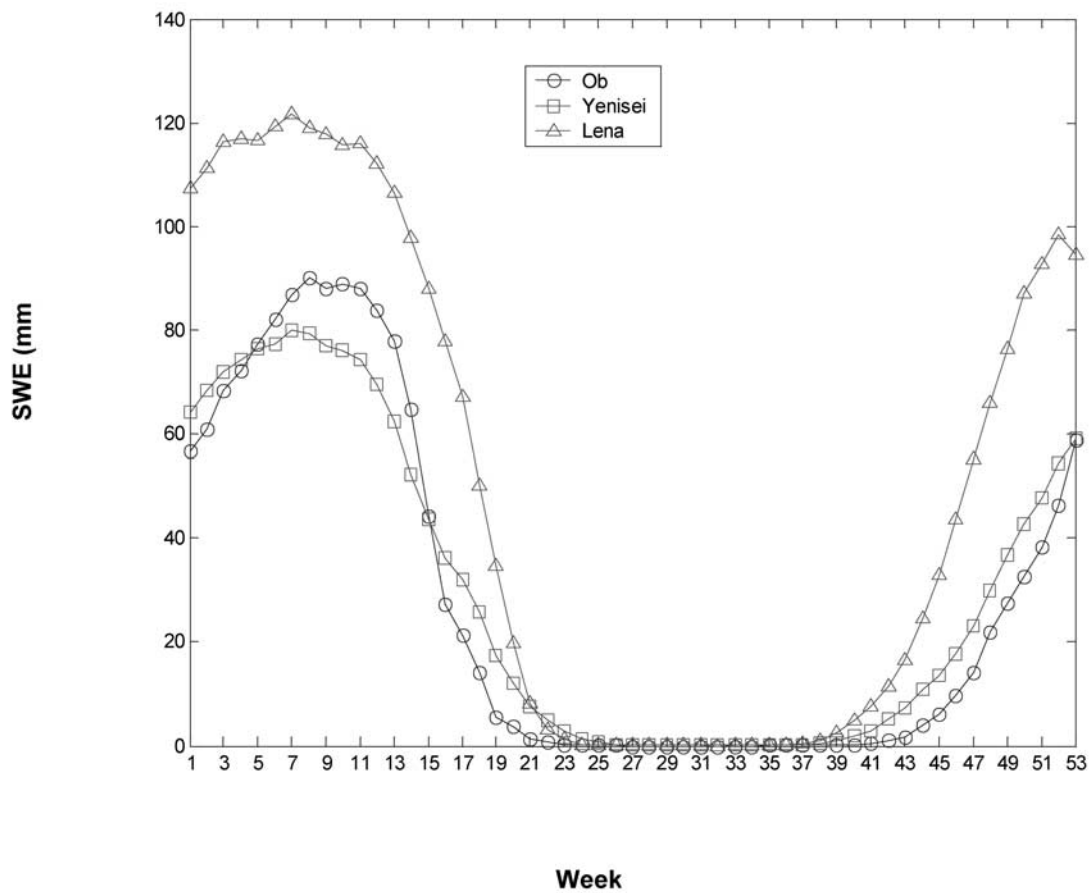


**Figure 2.** Mean weekly snow water equivalent (SWE, mm) over the three basins, 1988–2000.

and melt processes. To evaluate the compatibility of snow cover data over the large arctic watersheds, we compare weekly basin SWE data with weekly SCE, air temperature and winter precipitation. We also use a linear regression approach to define the weekly relationship between SWE and other variables.

#### 4.1. Basin SWE Versus SCE

[11] Comparisons of weekly basin SCE with SWE data from 1988 to 1999 show reasonable similarities in the SCE and SWE seasonal cycles (Figure 5), although noticeable differences exist particularly in the winter season. As expected, the basin SCE reaches 100% in early winter and maintains at this peak level throughout the winter season, while the basin SWE continues to increase until mid winter and then decreases slightly before the spring melt season starts. In the spring season, the basin SWE starts to decrease due to melt, while the basin SCE maintains at 100%. As the melt progresses, further reduction of the basin SWE leads to the SCE decrease in late spring. Both basin SCE and SWE reach zero during late spring to early summer when the basins become snow free.

[12] The general compatibility in the SCE and SWE seasonal cycles encourages applications of these data for large-scale hydroclimatic investigations. To further quantify the consistency between the SWE and SCE data, we compare respectively the beginning and ending dates of the snow cover season for the study period, and find a

general consistency in the SWE and SCE data. Most years both SWE and SCE show same weeks for start and end of the snow cover season, although they are slightly different (less than 2 weeks) in some years. The time differences between the maximum SWE and maximum SCE (at 100%) in the Lena River are larger than that for the Ob and Yenisei basins. This is mainly because of a higher maximum snow accumulation in the Lena basins relative to the Ob and Yenisei basins. Usually a thicker snowpack takes a longer time to melt to reduce the snow extent from 100% to an incomplete snow cover (i.e., SCE below 100%).

[13] Regression analyses of the weekly basin SWE versus SCE indicate positive relationships in a few weeks during the accumulation and melt seasons. It is important and useful to define these relationships, as they enable us to use the weekly SCE data to estimate the SWE values over the large arctic basins. Snow cover formation begins with the SCE increase and ends with the SWE peak. The early snow accumulation is dominated by the SCE increase, while the SWE remains very low. We found that in most accumulation weeks, the basin SCE and SWE do not correlate very well. Previous studies have shown that current passive microwave snow cover algorithms tend to underestimate snow cover extent over large areas during fall and early winter when snow is typically shallow and/or intermittent [Armstrong and Brodzik, 2001]. During shallow snow conditions microwave data consistently indicate less snow covered area than optical satellite data. This underestimate

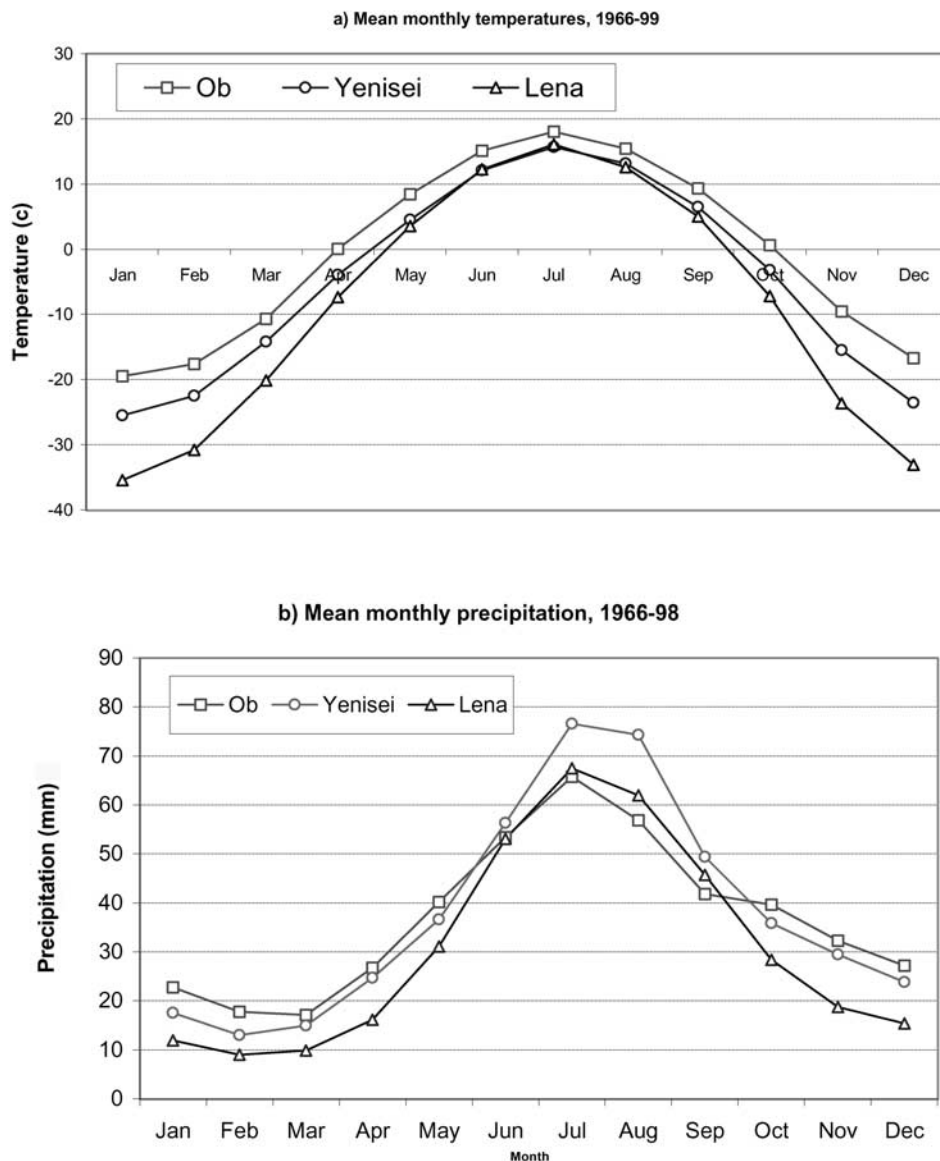


**Figure 3.** Long-term basin mean monthly (a) temperature (in °C) and (b) precipitation (in mm) over the three watersheds.

of snow cover extent results from at least two factors: (1) Shallow snow cover (less than about 5.0 cm) often possibly combined with wet snow does not provide a scattering signal of sufficient strength to be detected by the algorithms, and (2) even when snow cover exists at greater depths across the microwave sensor field of view but is intermittent in extent, the scattering signature integrated over this mixed pixel is not adequate to trigger current microwave algorithms [Armstrong and Brodzik, 2001, 2002].

[14] Over the winter season, the SCE remains at 100%, the SWE increases to the peak accumulation, and then decreases slightly without impacting the basin SCE. This study did not discover significant relationships between weekly basin SCE and SWE in winter season. During the snowmelt season, we detected positive relationship between basin SCE and SWE. This is reasonable as decreases in the SCE are associated with the decreases in SWE due to melt

of snowpack. Armstrong and Brodzik [2001] found that the SWE data accuracy increase during spring melt period. This is fortunate since spring is the most important period of the snow cover season in terms of snow hydrology, and a better quality of SWE data allows confident application to hydrologic forecasting and modeling [Armstrong and Brodzik, 2001].

**4.2. Basin SWE Versus Winter Precipitation**

[15] Figure 6 compares the basin SWE with the accumulated precipitation (AP) when the basin mean weekly temperatures are below 0°C. The accumulated precipitation may include rainfall events in early spring and late fall seasons particularly over the southern parts of the watersheds. The contribution of rainfall events is small to the winter total precipitation. Figure 6 shows high/low AP winters associated with similar SWE amounts among the

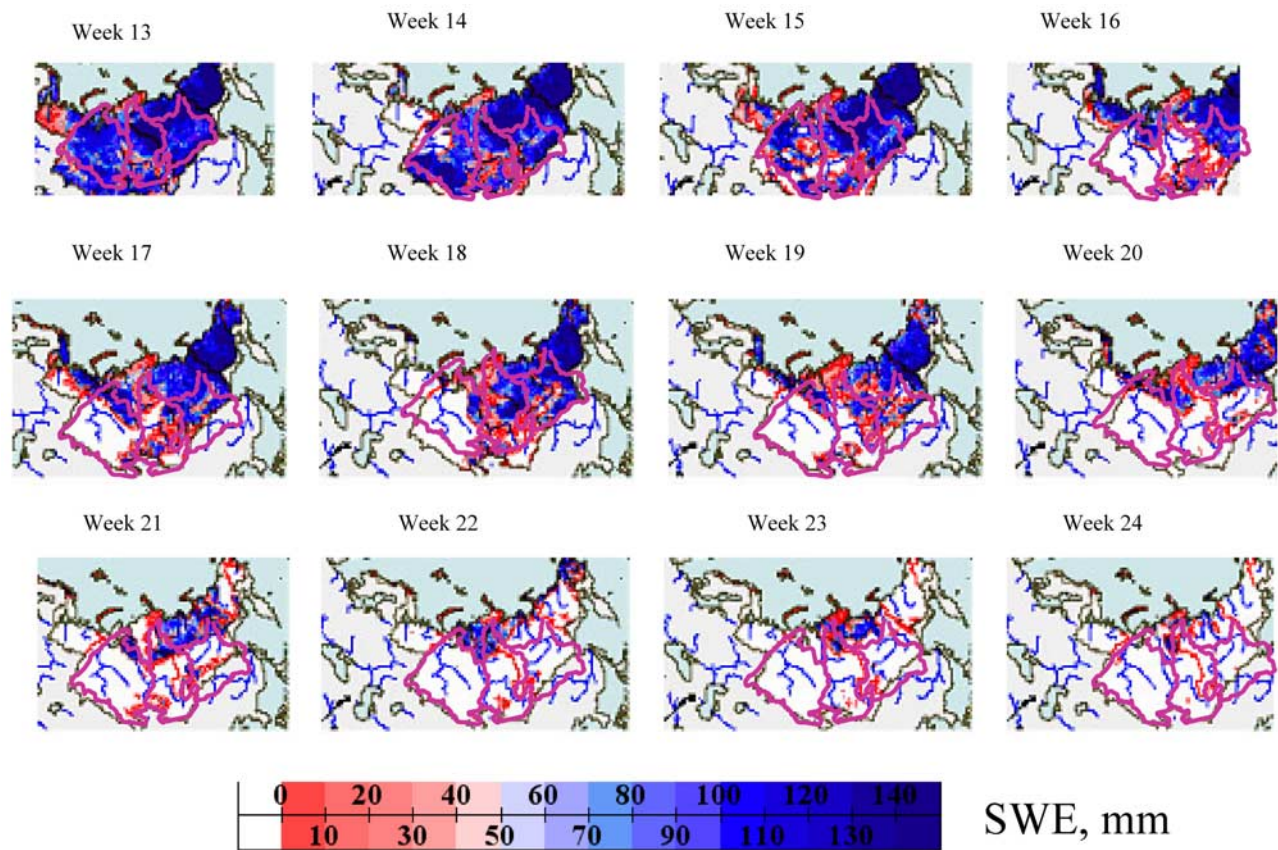


**Figure 4.** Changes of snow water equivalent (SWE, mm) over Siberia, during weeks 13–24, 1991. Also shown are river basin boundaries.

years, although in most years the basin SWE is generally less than the AP during snow cover season. It is interesting to note that the amounts of maximum SWE are closer to AP in low snowfall winters and much less than AP in high-snowfall winters. It is reasonable to expect that basin maximum SWE should be generally close to winter total snowfall amount. The lack of correspondence of the basin SWE to AP variation indicates some inconsistency between the SWE and precipitation data. This is not completely unexpected given the large biases in precipitation data over the high-latitude regions [Yang *et al.*, 2005; Yang and Ohata, 2001] and limitations in remote sensing snow cover algorithm [Armstrong and Brodzik, 2001; Walker and Goodison, 1993]. In addition, sublimation loss from snowpack over winter is another factor contributing to the uncertainty in SWE and AP compatibility. Studies reported that sublimation from the snow surface accounts for up to 1/3 of total accumulation in the northern regions [Benson, 1982; Benson and Sturm, 1993; Liston and Sturm, 1998, 2004; Pomeroy *et al.*, 1993]. Sublimation over large basins and regions is difficult to determine through direct measurements. Snow models taking into account of blowing and drifting snow processes can provide reasonable estimate of regional winter sublimation amount [Liston and Sturm, 1998, 2002; Pomeroy *et al.*, 1993].

[16] The ratios of maximum basin SWE versus AP are 17–80% (mean 47%) for the Ob basin, 30–66% (mean 53%) for the Yenisei basin, and 96–177% (mean 122%) for

the Lena watershed. The ratios close to 100% reflect less difference between the SWE and AP. The interannual variations in the SWE/AP ratios are mainly due to fluctuations in snowfall amounts and temperatures over the winter season. The low (high) ratios are found associated with high (low) AP and warm (cold) winter. It is interesting to note that, relative to other basins, the Lena basin SWE/AP ratios are particularly higher. This seems reasonable, as the climate in the Lena basin is colder (Figure 3a) and winter snow cover there has less potential sublimation and melt losses. However, we even found that the Lena basin SWE was greater than the AP for most years. This unexpected result indicates uncertainties in the SWE and AP estimations over the Siberian regions. Precipitation gauge undercatch of snowfall may be a factor, since Yang and Ohata [2001] found underestimation of yearly precipitation by 25–50% in the northern Lena regions. In addition, determination of timing of snow cover accumulation is also a challenge. In this study, basin mean temperatures at 0°C were used to estimate the beginning date (week) of snow cover formation, i.e., the starting point for accumulating precipitation (AP). Given the very large size of the watersheds, basin mean temperatures do not always represent the thermal conditions over the entire basin, particularly during spring and fall transition periods. Because of colder temperatures in the northern parts of the basin during fall season, snow cover starts to accumulate there early even when the basin mean temperatures are slightly above 0°C. This may lead to

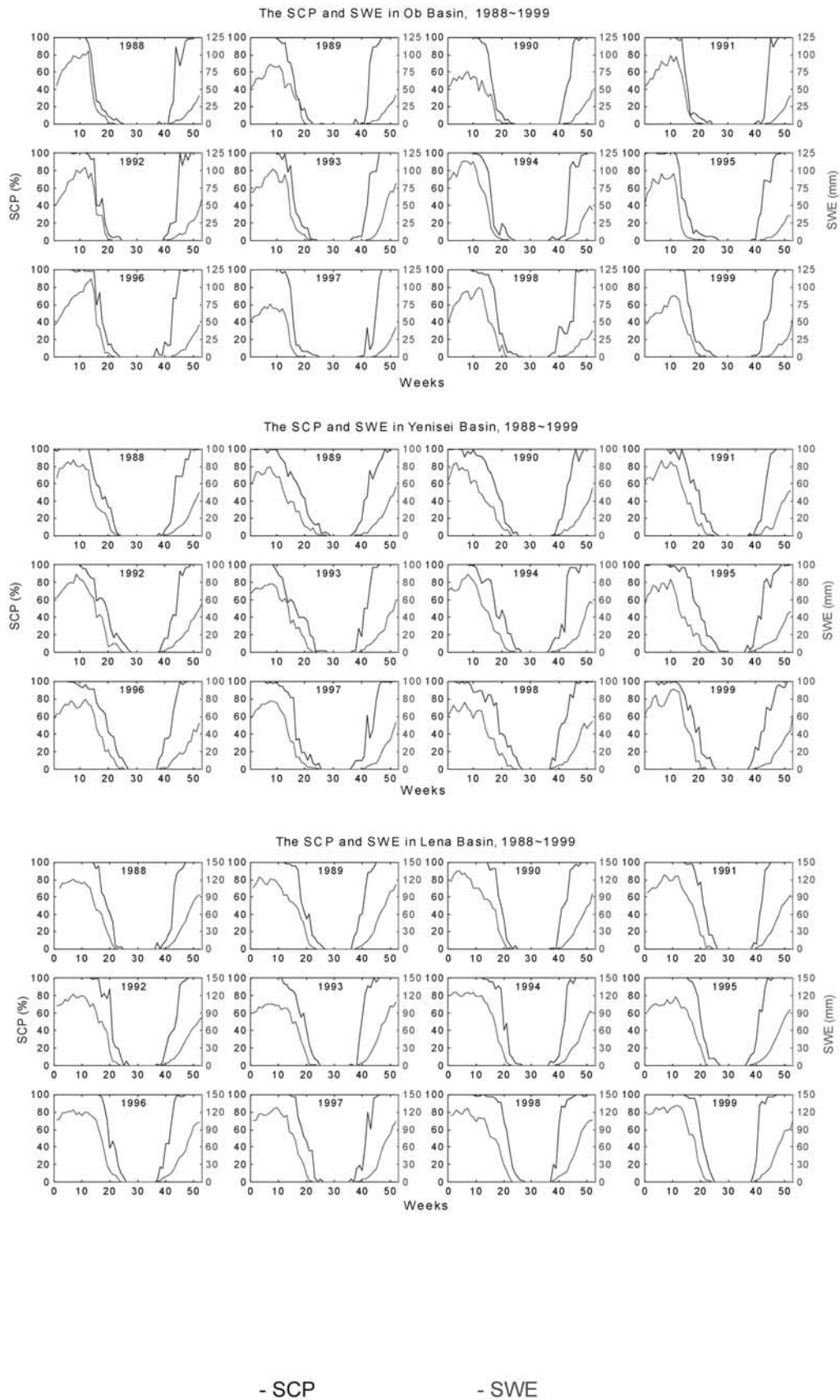
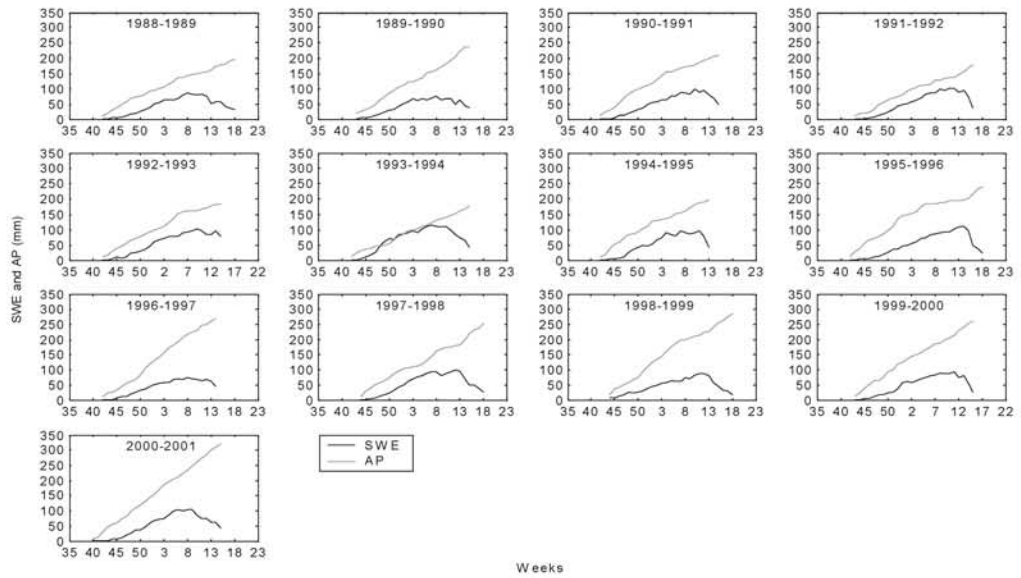
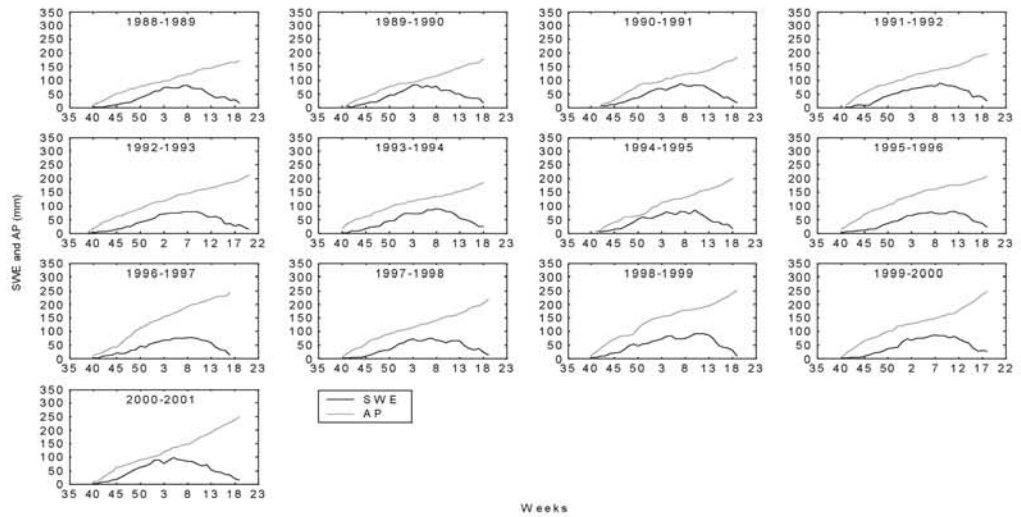


**Figure 5.** Comparisons of basin snow cover percentage (SCP, %) with basin snow water equivalent (SWE, mm) for the basins during 1988–1999.

a) Ob



b) Yenisei



c) Lena

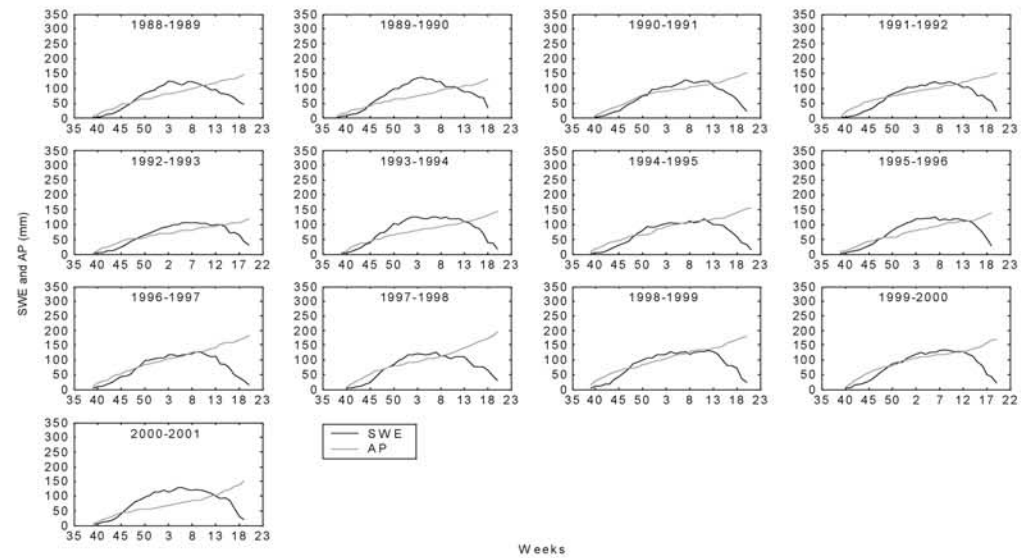
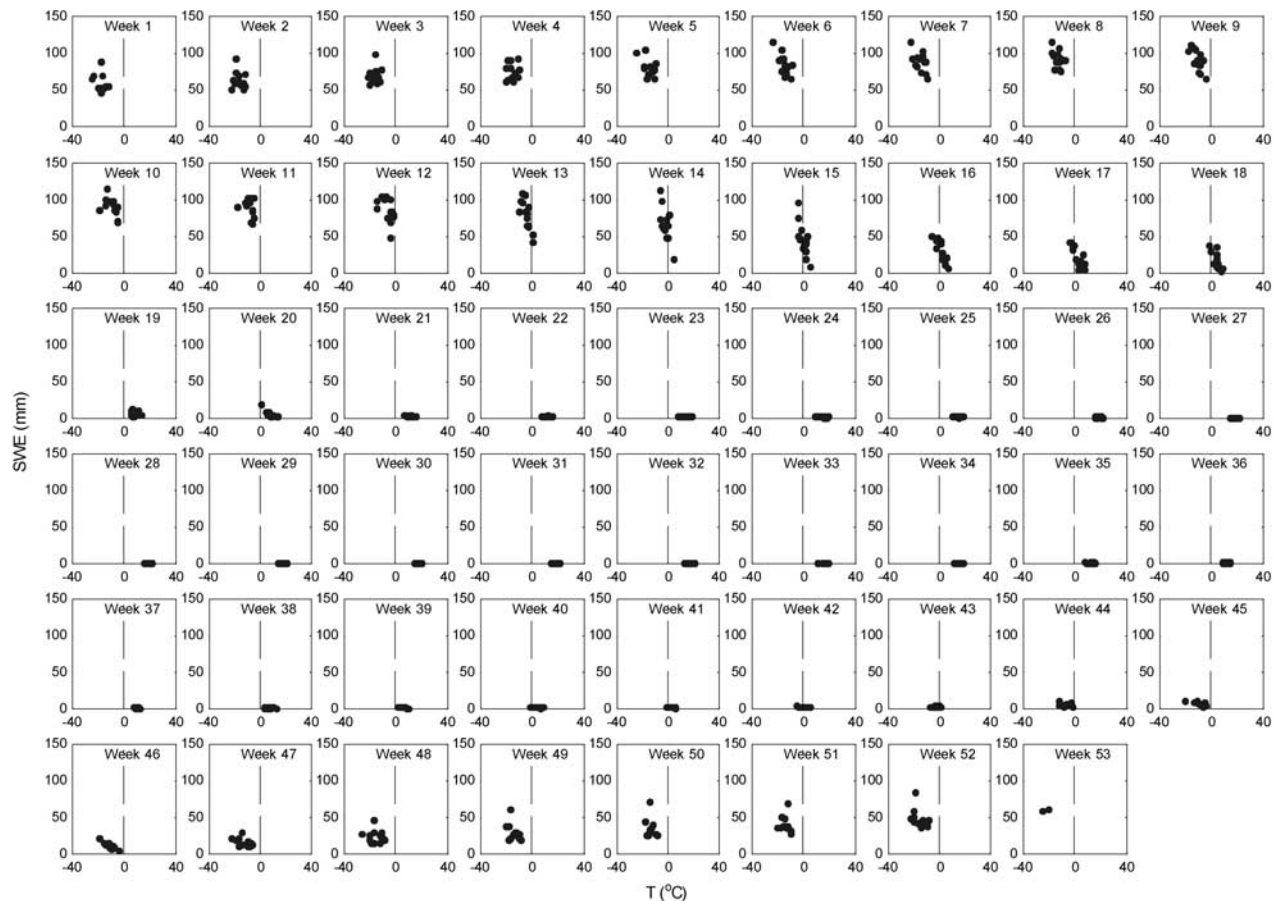


Figure 6. Comparisons of basin snow water equivalent (SWE, mm) with winter accumulated precipitation (AP, mm) for the basins during 1988–1999.



**Figure 7.** Ob basin scatterplots of weekly snow water equivalent (SWE, mm) versus weekly air temperature ( $^{\circ}\text{C}$ ) for the 53 weeks in a year during 1988–1999.

an underestimate of the basin AP for the basins, particularly for the Lena River due to a greater precipitation gradient over the eastern Siberian regions.

#### 4.3. Basin SWE Versus Temperature

[17] To examine and quantify the impact of temperature on basin SWE, a linear regression is applied to the temperature and SWE data sets for each week in a year (Figures 7–9). The results generally show that the SWE changes as a function of temperature. The basin SWE is the highest in the beginning of the year when temperatures are very cold between  $-15^{\circ}\text{C}$  and  $-30^{\circ}\text{C}$ . Snow cover mass decreases in spring from very high to very low in a short time when basin temperatures are around  $0^{\circ}\text{C}$ . The basins are snow-free in the short summer season. Snow cover forms when temperatures drop back to around  $0^{\circ}\text{C}$  in fall and continues to accumulate over the fall-winter seasons. Regression analyses identify strong negative correlations between basin SWE and temperatures, particularly when temperatures are close to  $0^{\circ}\text{C}$  during the snow accumulation and melt seasons (Table 1). These correlations demonstrate the association of (high) low SWE with (low) high temperatures.

#### 5. Seasonal Cycle of Streamflow

[18] The seasonal cycle of discharge at the basin outlets is illustrated in Figure 10. It generally shows the similar

features across Siberia: low flow during November to April (weeks 45–17) and high flow from June to October (weeks 23–43), with the maximum discharge occurring usually in June (weeks 23–26) due to snowmelt runoff. It also indicates noticeable differences in streamflow characteristics between the basins mainly due to different climate and permafrost conditions over the Siberian regions.

[19] Snowmelt causes the river streamflow to increase at week 17 in both the Ob River and the Yenisei watersheds, and week 20 (the second week in May) in the Lena catchment, respectively. The early rise of discharge in the Ob River is associated with the early melt of snow cover over western Siberia (Figures 2 and 4). As snowmelt progresses, discharge continues to rise in these watersheds. In comparison to the Ob River, the rates of streamflow rise are very high in the Yenisei and Lena basins, up to  $38,000\text{ m}^3/\text{s}$  and  $40,000\text{ m}^3/\text{s}$  per week, respectively. As a result, the Lena River reaches to the peak streamflow in 3 weeks. Streamflow of the three rivers peaks at the same time, i.e., week 23–24 (or mid-June), when the basins are covered by a small patchy snowpack, i.e., approximately 4% SCE and 1 mm SWE in the Ob river, 22% SCE and 4mm SWE in the Yenisei basin, and 15% SCE and 2mm SWE in the Lena basin. The basin SWE amounts are very low at the time of peak streamflow, reflecting a long lag of streamflow response to snowmelt and flow routing within the large watersheds.

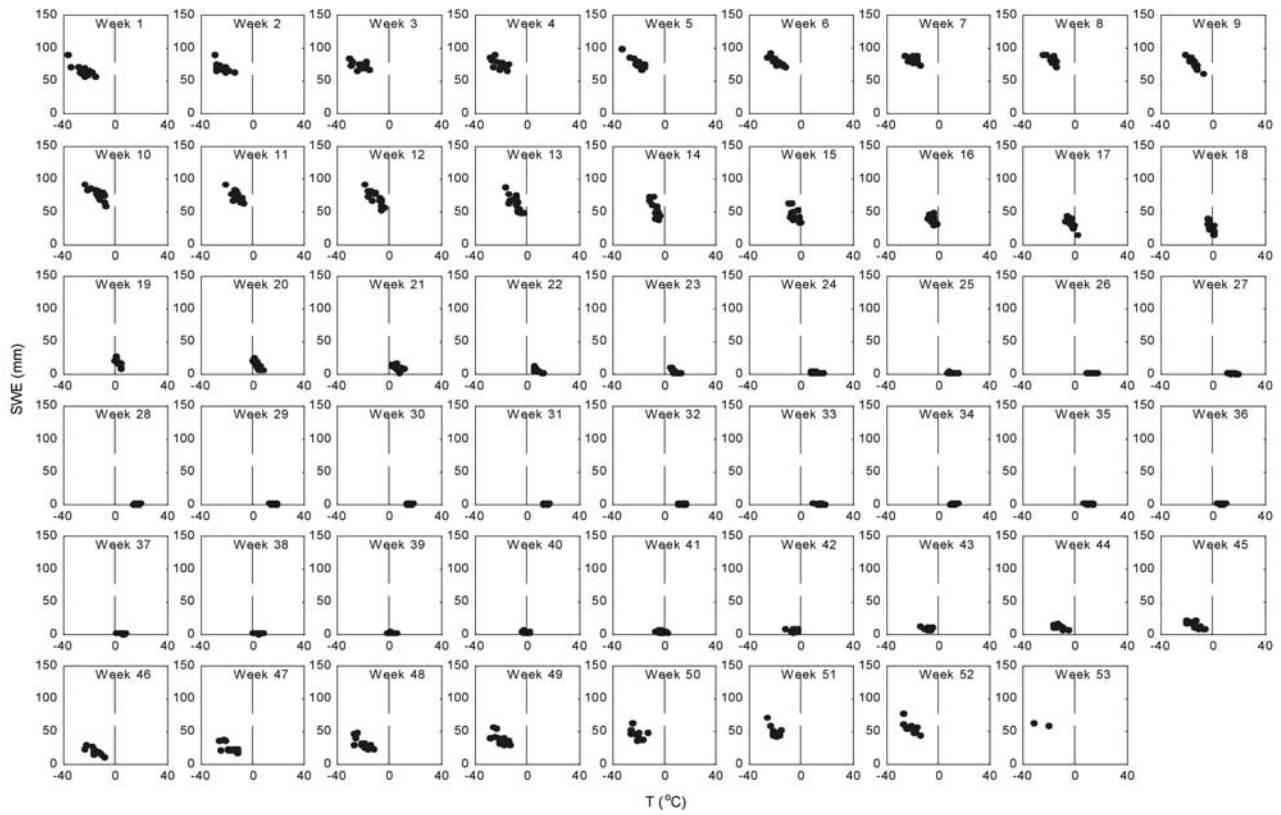


**Figure 8.** Yenisei basin scatterplots of weekly snow water equivalent (SWE, mm) versus weekly air temperature ( $^{\circ}\text{C}$ ) for the 53 weeks in a year during 1988–1999.

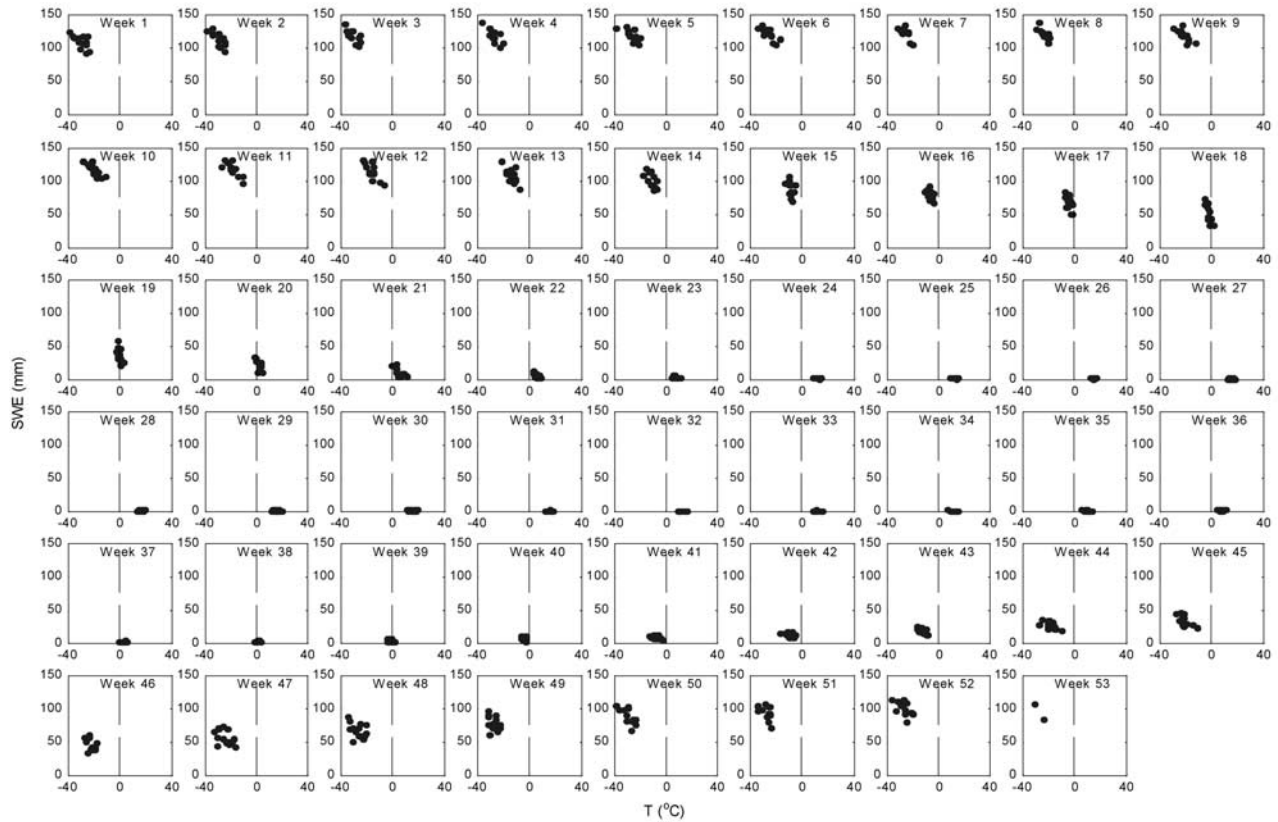


**Figure 9.** Lena basin scatterplots of weekly snow water equivalent (SWE, mm) versus weekly air temperature ( $^{\circ}\text{C}$ ) for the 53 weeks in a year during 1988–1999.

**Table 1.** Summary of Statistically Significant (85% Confident) Regression Results During the Snowmelt Weeks, 1988–2000

Week	Ob Basin		Yenisei Basin		Lena Basin	
	Regression Equation	R <sup>2</sup>	Regression Equation	R <sup>2</sup>	Regression Equation	R <sup>2</sup>
<i>Snow Water Equivalent (SWE, mm) Versus Air Temperature (T, °C)</i>						
12	SWE = 73.215-1.894 T	0.259	SWE = 50.372-1.922 T	0.713	SWE = 79.622-2.111 T	0.637
13	SWE = 59.018-4.837 T	0.570	SWE = 40.374-2.442 T	0.643	SWE = 79.222-2.058 T	0.493
14	SWE = 57.857-5.375 T	0.458	SWE = 27.371-3.943 T	0.702	SWE = 73.448-2.415 T	0.486
15	SWE = 47.288-6.594 T	0.628	SWE = 33.138-2.135 T	0.412	-	-
16	SWE = 35.730-3.303 T	0.717	SWE = 31.635-1.142 T	0.165	SWE = 67.905-1.670 T	0.255
17	SWE = 29.233-2.943 T	0.685	SWE = 24.427-2.412 T	0.671	SWE = 55.767-2.878 T	0.267
18	SWE = 30.270-3.135 T	0.636	SWE = 23.599-2.607 T	0.410	SWE = 40.865-5.221 T	0.612
19	-	-	SWE = 23.924-2.881 T	0.756	SWE = 35.275-3.479 T	0.271
20	SWE = 13.363-1.071 T	0.584	SWE = 21.545-2.173 T	0.729	SWE = 26.561-2.423 T	0.327
21	SWE = 3.409-0.185 T	0.215	SWE = 13.793-0.911 T	0.320	SWE = 16.241-1.337 T	0.398
22	-	-	SWE = 14.136-1.224 T	0.567	SWE = 10.999-1.098 T	0.610
23	-	-	SWE = 11.658-0.948 T	0.613	SWE = 6.0524-0.521 T	0.405
<i>Discharge (Q, m<sup>3</sup>/s) Versus Snow Water Equivalent (SWE, mm)</i>						
16	Q = 5.939-0.061 SWE	0.407	-	-	-	-
17	Q = 6.894-0.098 SWE	0.598	Q = 13.475-0.097 SWE	0.239	-	-
18	Q = 9.389-0.189 SWE	0.529	Q = 19.119-0.268 SWE	0.212	-	-
19	Q = 16.928-1.085 SWE	0.345	-	-	-	-
20	Q = 18.250-0.832 SWE	0.322	-	-	Q = 8.069-0.202 SWE	0.302
21	Q = 30.237-5.042 SWE	0.276	Q = 78.617-4.002 SWE	0.446	Q = 33.481-1.740 SWE	0.277

[20] The weekly (mean) peak streamflows range approximately from 35,000 m<sup>3</sup>/s for the Ob River to about 92,000 m<sup>3</sup>/s for both the Yenisei and Lena Rivers. Streamflow decreases at the end of the snowmelt season, although summer heavy rainfall events generate floods over the basins. The rate of discharge decrease is much slower in the Ob River than the Lena and Yenisei Rivers. Discharge reaches a minimum of 1600 m<sup>3</sup>/s during weeks 17–18 for the Lena River, 3,600 m<sup>3</sup>/s around weeks 14–15 for the Ob River, and 7,400 m<sup>3</sup>/s during 49–50 for the Yenisei River. Watersheds with high permafrost coverage generally have

low subsurface storage capacity and a low winter runoff and a high summer peak flow [Woo, 1986; Kane, 1997]. The Lena river, underlain by continuous permafrost (80–90%), has a very low winter flow and a very high peak flow in June, about 55 times greater than the minimum discharge. The Yenisei River, with 60–70% permafrost, shows a highest winter and peak flow, with about an eightfold increase over the minimum discharge in April. On the other hand, the Ob basin with about 30–40% permafrost coverage has the lowest peak discharge, about half of the other two rivers or ninefold the winter minimum runoff. The

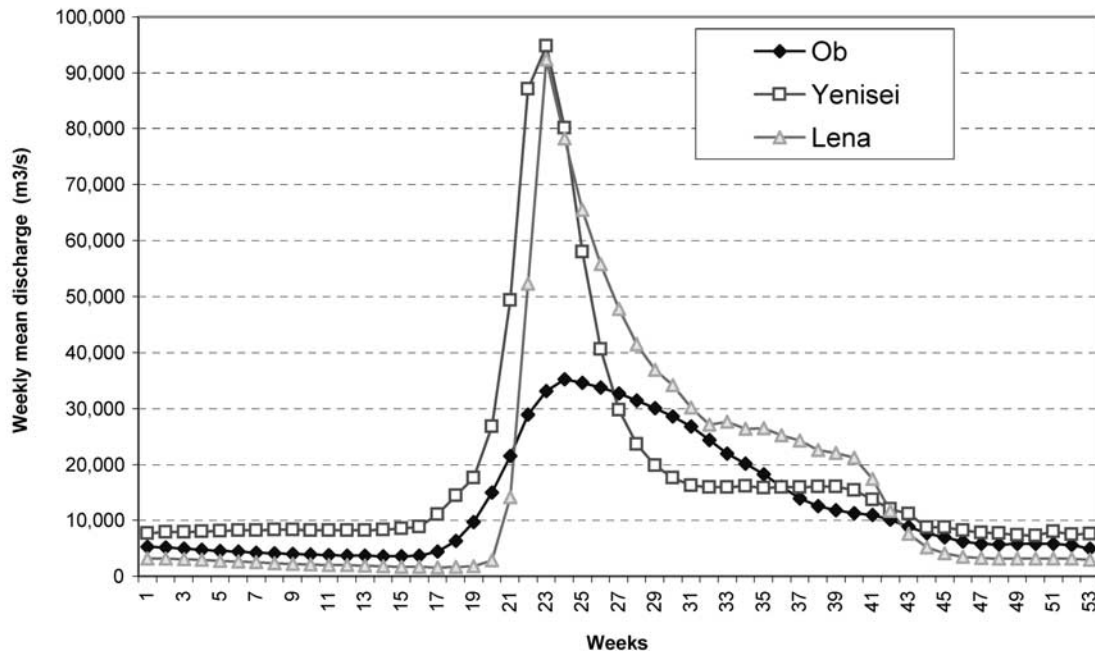
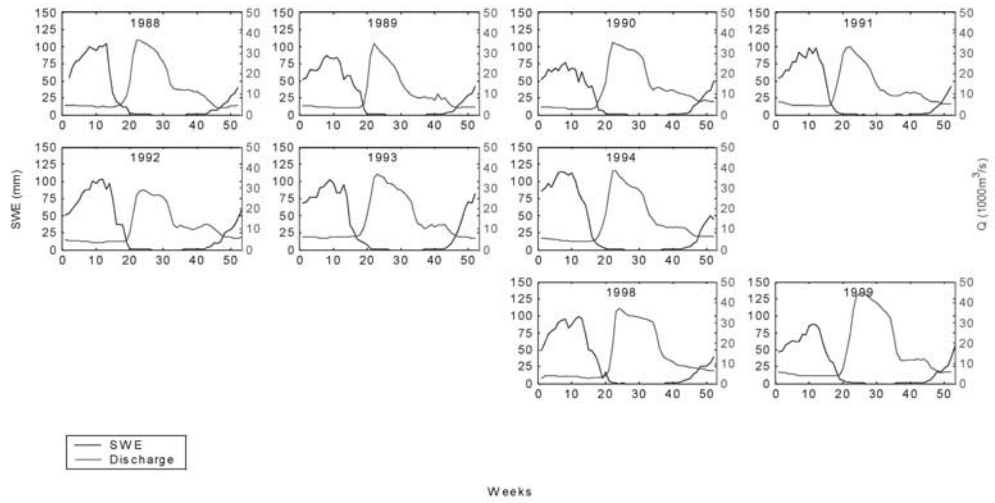
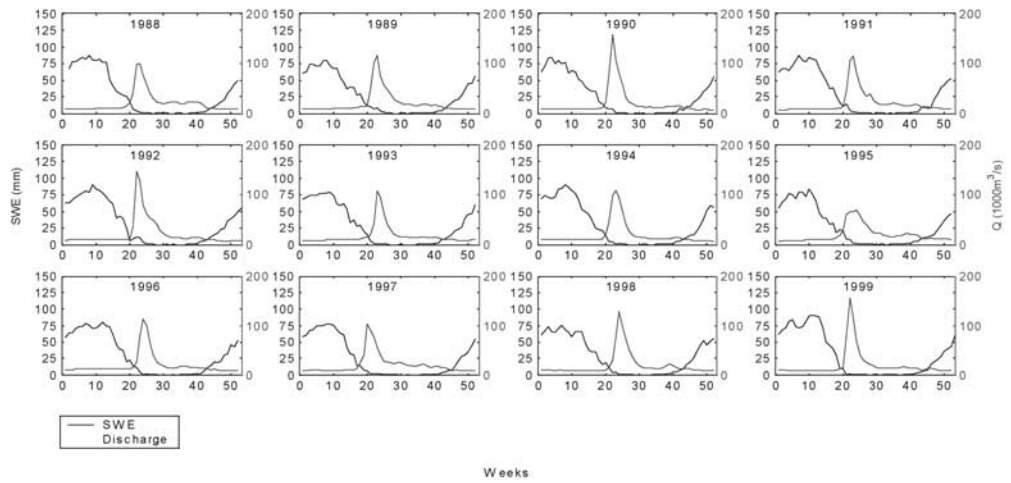


**Figure 10.** Mean weekly discharge (m<sup>3</sup>/s) at the basin outlets of the three large rivers, 1988–1999.

**a) Ob basin**



**b) Yenisei basin**



**c) Lena basin**

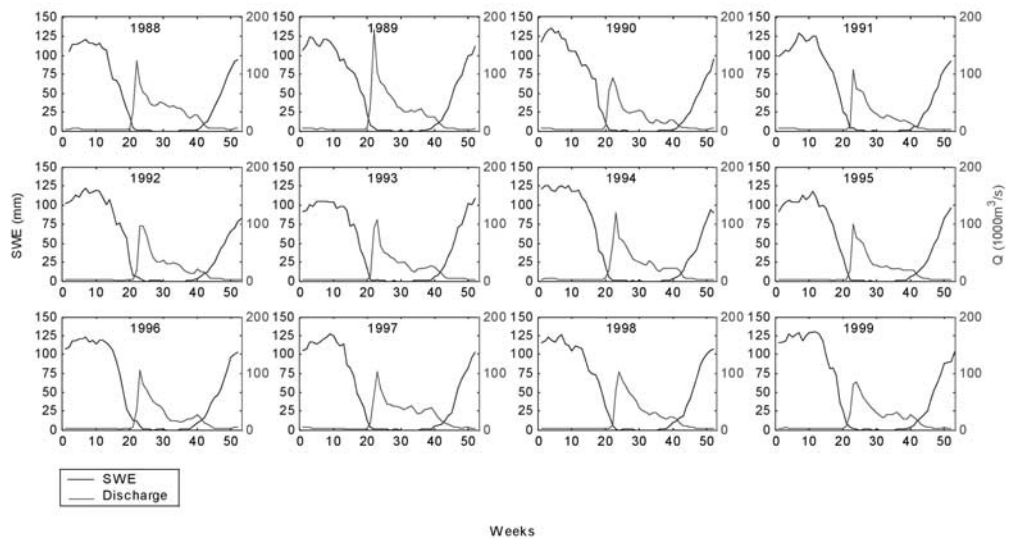


**Figure 11.** Comparisons of basin snow water equivalent (SWE, mm) with river discharge ( $Q, m^3/s$ ) for the basins during 1988–1999.

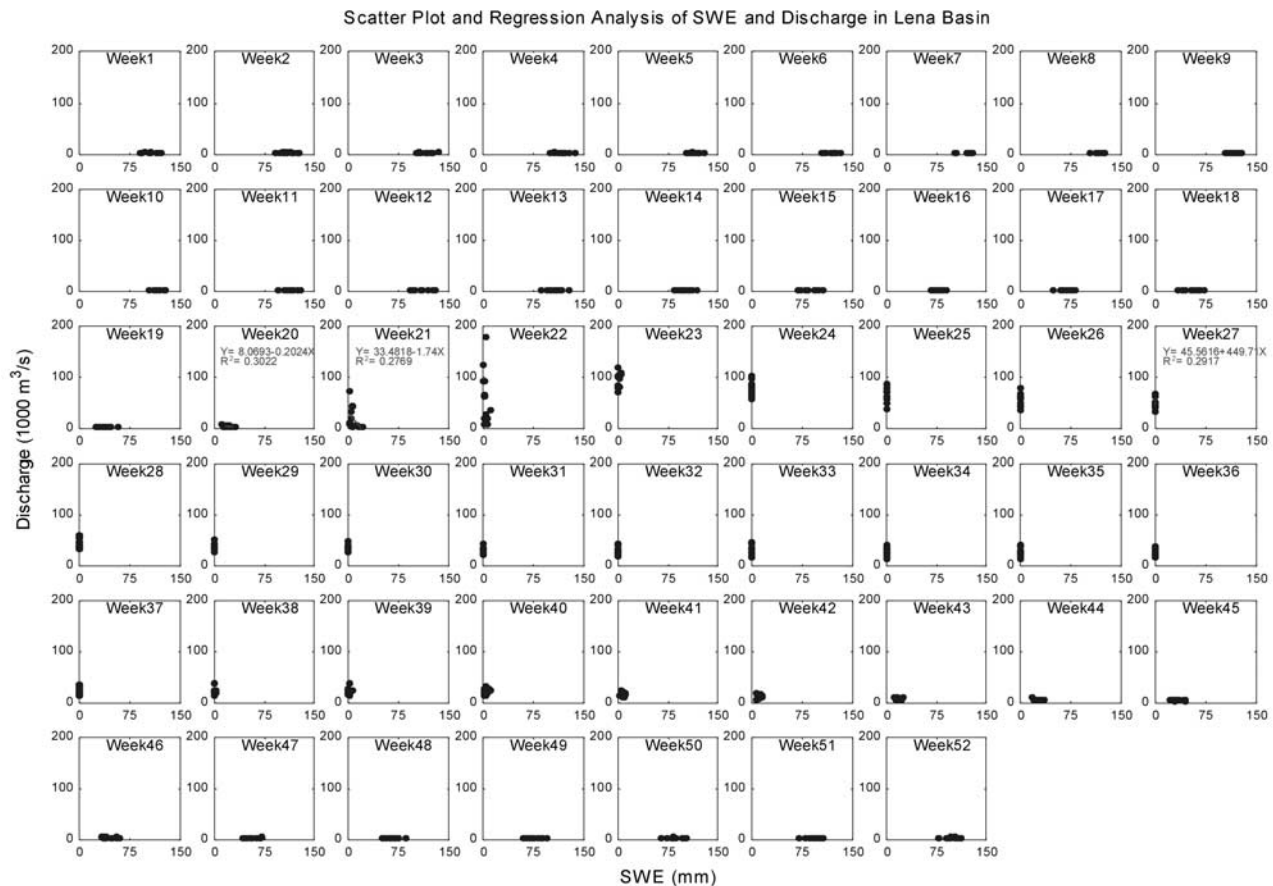


**Figure 12.** Lena basin scatterplots and regression equations of weekly discharge ( $Q$ ,  $\text{m}^3/\text{s}$ ) versus snow water equivalent (SWE, mm) for the 53 weeks in a year, 1988–1999.

quicker responses of streamflow to snowmelt and faster decrease of streamflow after snowmelt in the Lena and Yenisei rivers are also related to a lower subsurface storage capacity due to a higher percentage of permafrost coverage in central and eastern Siberian regions. The interannual variations of weekly streamflow are generally small in the cold season and large over summer months mainly due to rainfall storm activities and associated streamflow fluctuations.

## 6. Weekly Relation Between Streamflow and Basin SWE

[21] The seasonal changes of the basin SWE and streamflow in each individual year are displayed in Figure 11 for the three basins. They clearly indicate a general response of river discharge to seasonal snow cover changes over the Siberian regions, i.e., an association of low streamflow with high basin SWE during the cold season, and an increase in discharge associated with a decrease of the basin SWE during the melt periods. They also show the interannual variations in both SWE and streamflow. Relative to the basin SWE, streamflow varies much more between years. For instance, the Yenisei River peak streamflows were low ( $69,000 \text{ m}^3/\text{s}$ ) in 1995 and high ( $157,000 \text{ m}^3/\text{s}$ ) in 1990, while the maximum basin SWE were very close to each other (about 80–85 mm) for these 2 years. Similar cases

exist in other basins, such as 1989 (high peak flow) versus 1999 (low peak flow) for the Lena River, and 1992 (low peak flow) versus 1999 (high peak flow) in the Ob watershed. This discrepancy between basin snow cover and streamflow variations may suggest uncertainties in basin SWE data perhaps due to algorithm limitations [Armstrong and Brodzik, 2002].

[22] To quantify the response of river streamflow to basin snow cover variation, we examine and compare the weekly mean streamflow with the weekly basin SWE for the study period 1988–1999. The results generally confirm a meaningful relation between the streamflow and SWE during the spring melt season over the large Siberian watersheds (Figures 12–14). In the early melt period (weeks 12–16), Lena basin SWE reduces from 110 to 80 mm (Figure 12). Most of the meltwater is stored in ponds, lakes and river valleys. River ice breaks up around this time in the upper parts of the basin, but streamflow at the basin outlet does not show a clear response due to ice jams in the river valleys. As snowmelt progresses (weeks 17–20), SWE decreases from 70 to 10 mm, releasing more water to satisfy the surface storage within the basin. During weeks 21–22, river channels open up in the northern parts of the watershed and discharge at the basin mouth starts to rise. This response of streamflow to snowmelt is reflected by a negative correlation between streamflow and basin SWE in weeks 20–21.

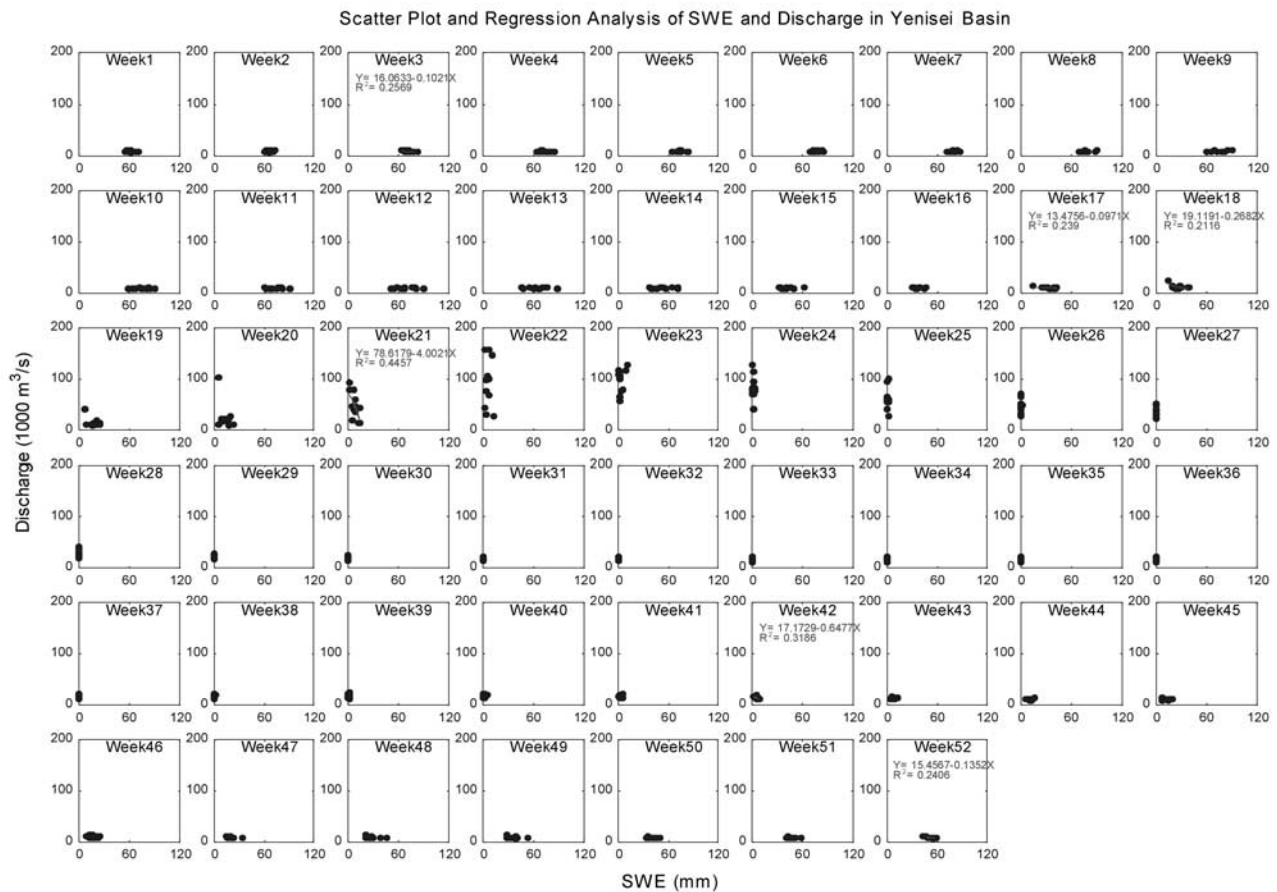


**Figure 13.** Yenisei basin scatterplots and regression equations of weekly discharge ( $Q$ ,  $\text{m}^3/\text{s}$ ) versus snow water equivalent (SWE, mm) for the 53 weeks in a year, 1988–1999.

In the late melt period (weeks 23–25), streamflow response to snowmelt weakens due to reduced snowmelt runoff contribution. Similar processes exist for the Yenisei basin. The strongest weekly relation between discharge and basin SWE is seen during weeks 17–18 and 21, when 25–45% of the basin is covered by a patchy snowpack (Figure 13). The Ob river streamflow significantly correlates with SWE during weeks 16–21, while basin SWE reduces from 30 to 5 mm (or about 33–36% of the maximum SWE) (Figure 14). The results of regression analyses are summarized in Table 1. They explain 20–60% of streamflow variability, although they are statistically significant at 85–95% confidence. It is useful to quantify these relationships, as they suggest a practical procedure of using remotely sensed SWE information for snowmelt runoff estimation over the large northern watersheds.

[23] In addition to the amount of end-of-winter SWE, rates of snow cover melt also affect runoff generation and streamflow process in the cold regions [Kane *et al.*, 2000; Yang *et al.*, 2003]. It is important to explore the relationship between snowmelt rate and streamflow variations between years for the large Siberian rivers. To do this, we calculate and compare the weekly SWE difference ( $\Delta\text{SWE} = \text{SWE} [\text{week } (n + 1) - \text{week } (n)]$ ) with weekly streamflow difference ( $\Delta Q = Q [\text{week } (n + 1) - \text{week } (n)]$ ) for the

three basins (Figures 15–17). The results generally show positive  $\Delta\text{SWE}$  during snow accumulation and negative  $\Delta\text{SWE}$  during snow ablation, and little change in  $\Delta Q$  during the low-flow season. There is no relation between these 2 variables in most weeks except in the snowmelt periods. A moderate negative relation exists between  $\Delta\text{SWE}$  and  $\Delta Q$  during snowmelt season, for instance, during weeks 20/21 to 22/23 for the Lena basin, weeks 19/20 to 21/22 over the Yenisei river, and weeks 16/17 to 19/20 for the Ob watershed. These results are consistent with those from Figures 12–14. The relation between  $\Delta\text{SWE}$  and  $\Delta Q$  during snowmelt periods indicates that fast (slow) melt of snowpack generates high (low) streamflow in the large watersheds. This is reasonable, as it reflects that energy available to snowpack affects interannual variations in snowmelt and streamflow processes.

## 7. Extreme SWE and Associated Streamflow

[24] The basin SWE and discharge data show that weekly snow cover and snowmelt peak flows vary significantly among years. To understand the variability in snowmelt runoff, it is necessary to examine extreme snow cover condition, its melt processes, and effect to snowmelt runoff generations. Two example years of highest and lowest SWE

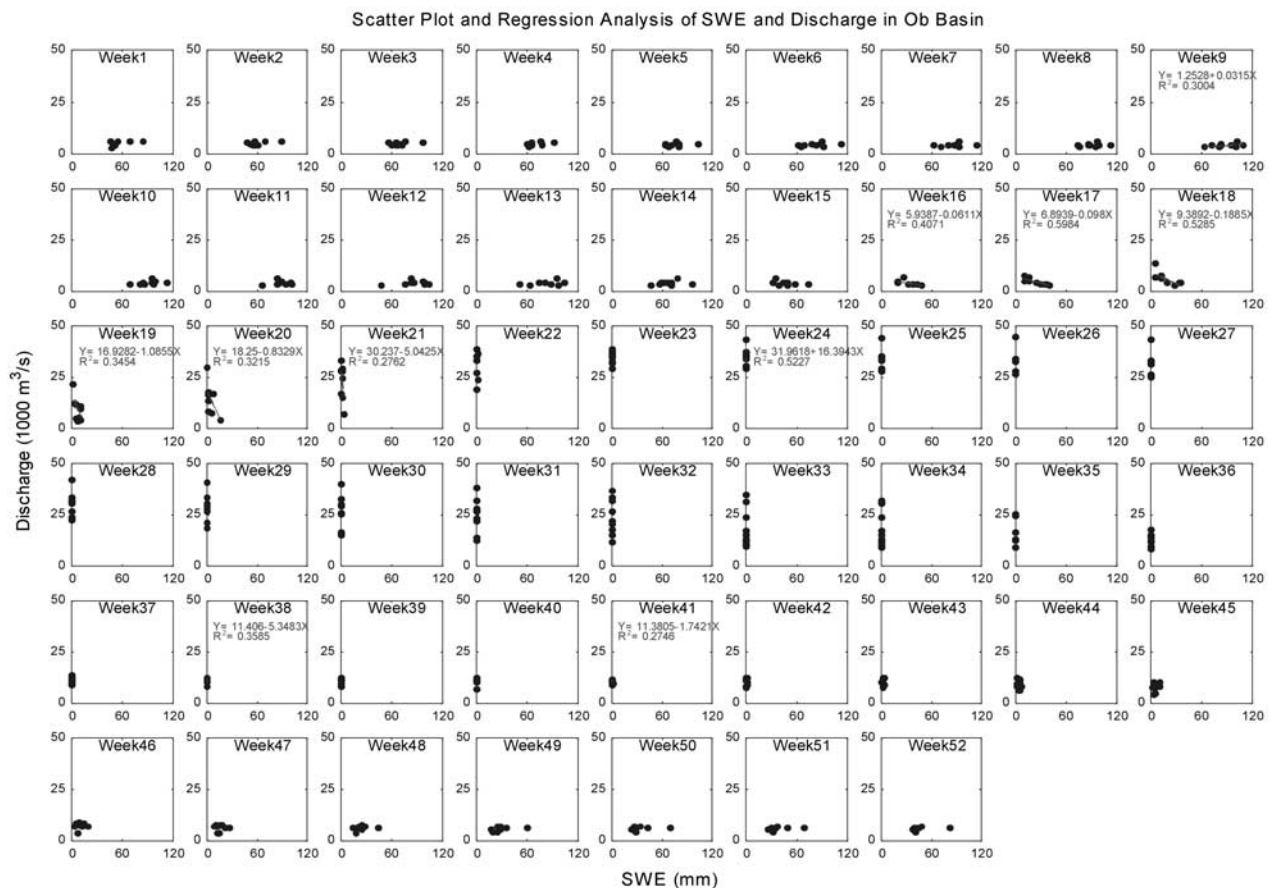


**Figure 14.** Ob basin scatterplots and regression equations of weekly discharge ( $Q$ ,  $\text{m}^3/\text{s}$ ) versus snow water equivalent (SWE, mm) for the 53 weeks in a year, 1988–1999.

cases were selected for each watershed in this analysis (Figure 18).

[25] The Ob basin SWE is high (maximum accumulation 114 mm) in 1994 and low (maximum accumulation 77 mm) in 1990 (Figure 18a). Snow melted fast in the high SWE year and produced a higher peak flow. This higher peak, although occurred at the same time (week 22) as for the low SWE year, sustained longer during weeks 22–23, clearly reflecting basin response to a higher SWE in 1994. The snowpack melted late in the low SWE year of 1990 and generated a slightly lower peak flow. It is interesting to note that difference in peak flows is much smaller than the difference in basin SWE between the extreme years. This again may suggest inconsistency between basin SWE and streamflow, although basin surface characteristics and other hydrologic factors may be an issue as well. The record high and low spring floods were recorded in 1999 and 1967, respectively, for the Ob basin [Yang *et al.*, 2004a]. The highest SWE in spring of 1994 did not correspond with the highest peak flow in 1999. Basin SWE data are not available in 1967 to compare with the record low flow that year.

[26] For the Yenisei basin, the extreme SWE years are 1999 (maximum SWE 91mm) and 1998 (maximum SWE 76 mm) (Figure 18b). Relative to the low SWE year, snow in the high SWE year melted fast and generated high peak

flow. The peak flow appeared 2 weeks earlier in the high SWE year. The peak flow in 1999 is one of the highest records during 1935–1999 [Yang *et al.*, 2004b]. This highest flow matches the highest basin SWE in spring of 1999, and its earlier peak is due to a quick melt of a thicker snowpack. Snow cover melted slowly in the low SWE year of 1998 and produced a late, low peak flow. The highest and lowest flow years are 1990 and 1995, respectively, in the Yenisei basin during 1988–1999. They do not correspond with the extreme SWE years of 1998 and 1999.

[27] The Lena basin snow accumulation is high in 1990 (maximum SWE 136 mm) and low (maximum SWE 105 mm) in 1993 (Figure 18c). Snow cover usually reaches maximum accumulation at the end of winter. The high SWE years of 1990 was, however, different in the Lena watershed, as the basin SWE was the maximum in the mid winter (during late January to early February), and then gradually decreased by about 30 mm during mid February to early March maybe due to strong sublimation or early snowmelt in the upper parts of the basins. The SWE in 1990 was similar with the low SWE year of 1993 at the beginning of melt season. The melt patters were very similar in both 1990 and 1993. Snow started melt around week 11 and ended at the same time (week 20), although the peak flow was relatively higher and occurred

Lena basin

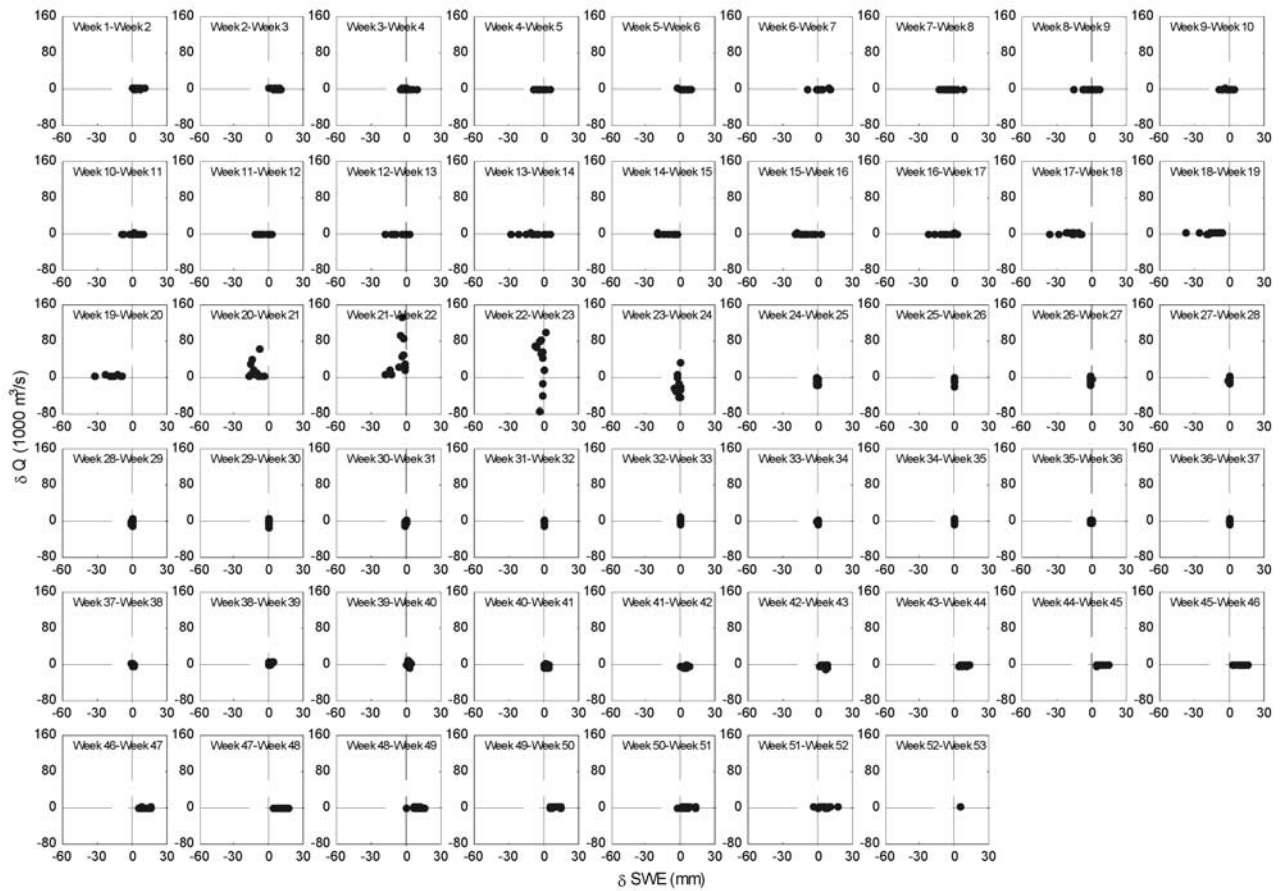


**Figure 15.** Scatterplots of Lena basin weekly discharge difference ( $\delta Q$ , m<sup>3</sup>/s) versus snow water equivalent difference ( $\delta$ SWE, mm) for the 53 weeks in a year, 1988–1999. Note “week1–week2” represents  $\delta Q$  and  $\delta$ SWE between week 2 and week 1.

## Yenisei basin

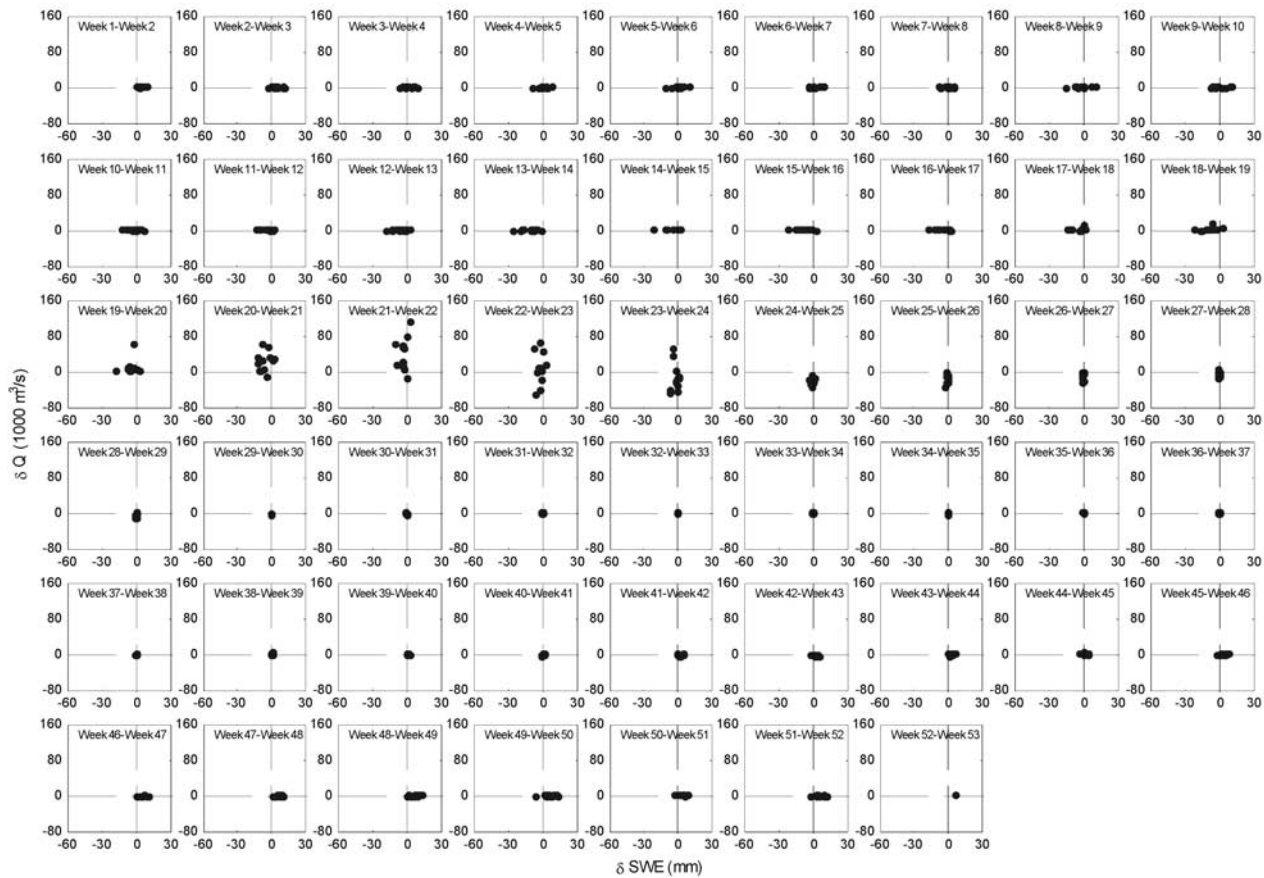


**Figure 16.** Scatterplots of Yenisei basin weekly discharge difference ( $\delta Q$ ,  $\text{m}^3/\text{s}$ ) versus snow water equivalent difference ( $\delta \text{SWE}$ , mm) for the 53 weeks in a year, 1988–1999.

later in 1993. The highest and lowest flows were registered in 1989 and 1999 during 1988–1999, respectively, for the Lena basin. They did not coincide with the extreme SWE years of 1990 and 1993.

[28] Overall, we identified noticeable differences in both peak flow amount and timing between the selected high/low SWE years in the large watersheds. The higher flows are sometimes associated with higher basin SWE. The differences between the high and low peak flows are, however, generally small relative to the normal interannual flow fluctuations. This suggests that, in addition to winter maximum SWE, other factors such as temperature and precipitation during the melt periods also affect snowmelt processes and influence the timing and magnitude of peak snowmelt floods. In addition, basin terrain features, surface and subsurface hydrologic characteristics, and soil properties will also affect snowmelt processes.

## 8. Conclusions

[29] Validation and evaluation of available remotely sensing products are important to develop our capability of

observing and monitoring the Earth system from the space. This study applied remotely sensed SWE, SCE and gridded climatic data to investigate snowmelt runoff response to seasonal snow cover change in the large Siberian watersheds. It defined the seasonal cycles and variations of snow cover mass and river streamflow, and identified a clear correspondence of river streamflow to seasonal snow cover mass change, i.e., an association of low streamflow with high snow cover mass during the cold season, and an increase in discharge associated with a decrease of snow cover mass during the melt periods. It also examined the compatibility of the basin SWE data with the SCE, peak snowmelt floods, and climatic variables (temperature and winter precipitation), and found consistency among the basin SWE, SCE and temperature. On the other hand, it detected incompatibility between basin SWE and winter precipitation for the Lena watershed, suggesting limitations in SWE retrieval algorithm and uncertainties in determination of basin winter snowfall amounts.

[30] To quantify the relation between river streamflow and basin snow cover variations, this study compared the weekly mean streamflow with the weekly basin SWE for

## Ob Basin

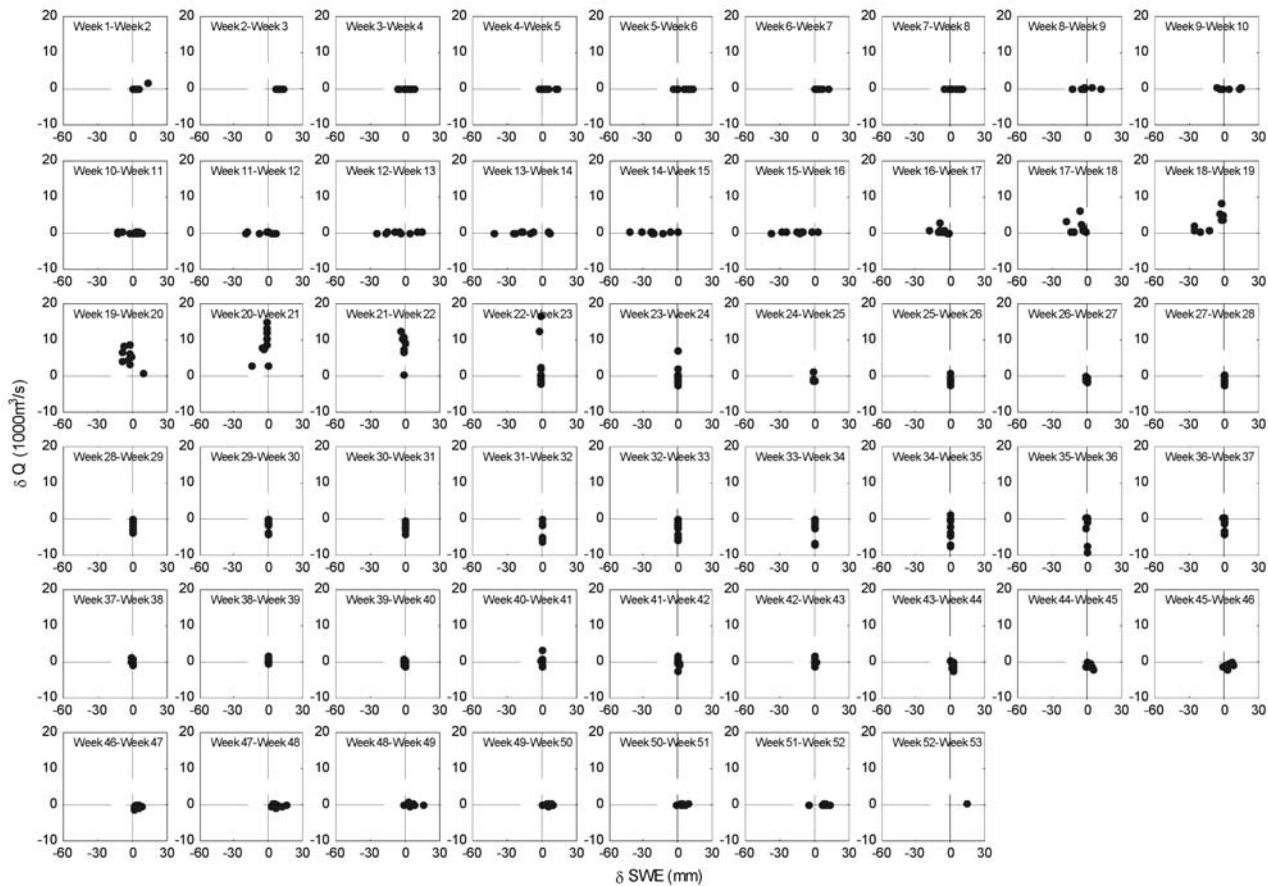
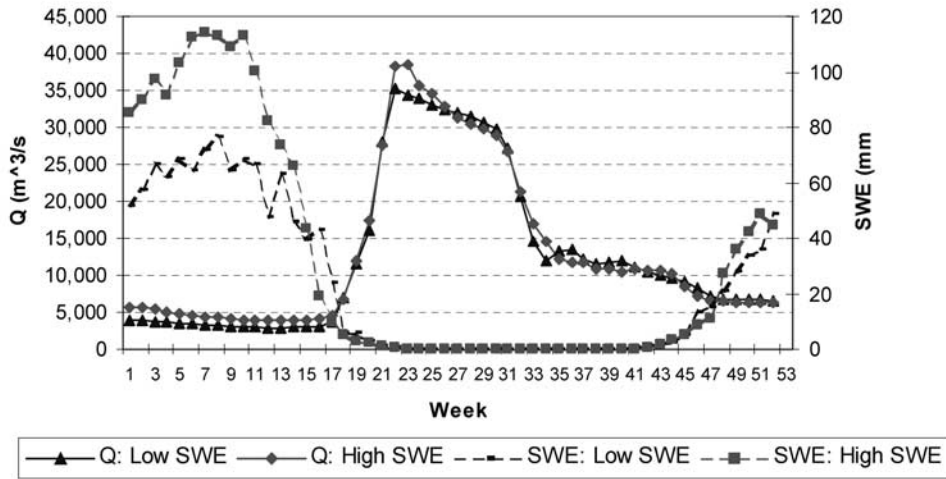


**Figure 17.** Scatterplots of Ob basin weekly discharge difference ( $\delta Q$ ,  $\text{m}^3/\text{s}$ ) versus snow water equivalent difference ( $\delta \text{SWE}$ , mm) for the 53 weeks in a year, 1988–1999.

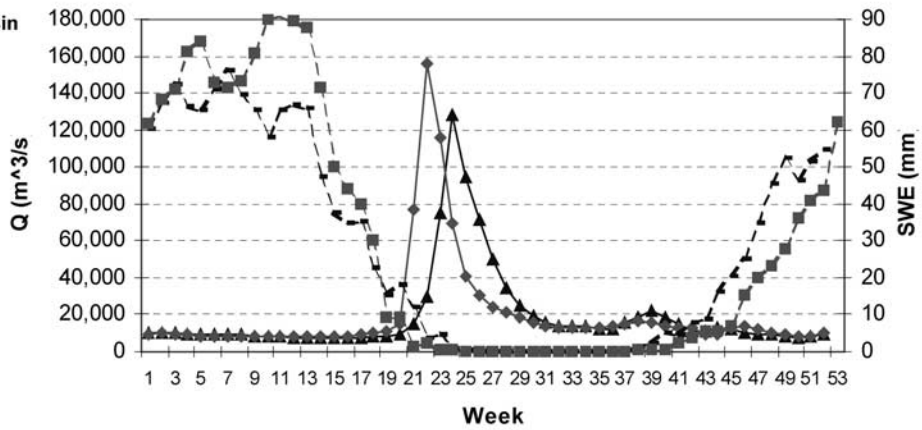
the study period (1988–2000). The results revealed a moderately strong linkage between streamflow and basin SWE during the spring melt season over the large Siberian watersheds and developed a statistically significant weekly streamflow–SWE relation. It is important to define these relationships, as they improve our understanding of the most important arctic hydrologic process—snowmelt peak floods, and they also suggest practical procedures of using remotely sensed snow cover information for snowmelt runoff forecasting over the large northern watersheds with insufficient ground observations. Furthermore, analyses of extreme (high/low) SWE cases (years) and the associated streamflow conditions indicate a general association of high (low) flow peak with high (low) maximum SWE in the river basins, although some inconsistencies exist between extreme flow and basin SWE. These results point to a need to further search for the best snowmelt–streamflow relationship, and to develop the most useful snowmelt runoff forecasting methods for the large northern rivers.

[31] The results of this study demonstrate that remote sensing snow cover data are useful in understanding streamflow characteristics and changes in the arctic regions with very sparse observational network. The methods and results of this research will be important to snowmelt model and process studies. They will improve our understanding of the spatial and temporal variability of high-latitude snow cover and its contribution to river runoff in the arctic regions. They will also enhance our capability of modeling cold region land memory processes and predicting future changes in water cycle over large northern regions. Snow depth and water equivalent data obtained by ground observations are also useful to better understand snowmelt runoff processes. Long-term snow observations particularly over the Siberian regions have been found valuable for cold region climate studies [Armstrong and Brodzik, 2001; Ye *et al.*, 1998]. There is a need to investigate the compatibility of the basin SWE with in situ snow cover observations. Our efforts are currently underway to compile and evaluate the high-latitude in situ snow cover data for northern hydrology investigations.

a) Ob basin



b) Yenisei basin



c) Lena basin

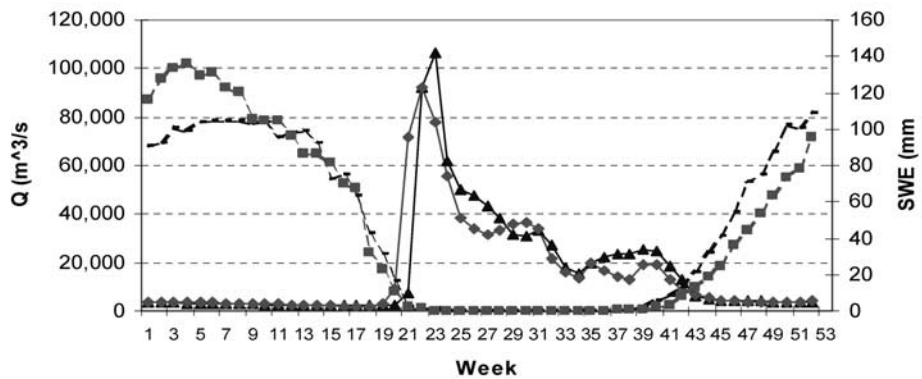


**Figure 18.** Comparison of extreme snow water equivalent (SWE, mm) and associated discharge ( $Q, m^3/s$ ) conditions over the three watersheds.

[32] **Acknowledgments.** This research was supported by the NSF grants ARC-0230083/ARC-0612334, NOAA/CIFAR grant NA17RJ1224, and NASA research grant NNG04GN38G.

## References

- Aagaard, K., and E. C. Carmack (1989), The role of sea ice and other fresh water in the arctic circulation, *J. Geophys. Res.*, *94*(C10), 14,485–14,498.
- Armstrong, R. L., and M. J. Brodzik (2001), Recent Northern Hemisphere snow extent: A comparison of data derived from visible and microwave sensors, *Geophys. Res. Lett.*, *28*(19), 3673–3676.
- Armstrong, R. L., and M. J. Brodzik (2002), Hemispheric-scale comparison and evaluation of passive microwave snow algorithms, *Ann. Glaciol.*, *34*, 38–44.
- Benson, C. S. (1982), Reassessment of winter precipitation on Alaska's Arctic slope and measurement on the flux of wind blown snow, report, 26 pp., Geophys. Inst., Univ. of Alaska Fairbanks, Fairbanks.
- Benson, C. S., and M. Sturm (1993), Structure and wind transport of seasonal snow on the Arctic slope, *Ann. Glaciol.*, *18*, 261–267.
- Brabets, T., B. Wang, and R. Meade (2000), Environmental and hydrologic overview of the Yukon river basin, Alaska and Canada, *U. S. Geol. Surv. Water Resour. Invest. Rep.*, *99-4204*, 106 pp.
- Brodzik, M. J., and K. W. Knowles (2002), EASE-Grid: A versatile set of equal-area projections and grids, in *Discrete Global Grids*, chap. 5, edited by M. Goodchild and A. J. Kimerling, Natl. Cent. for Geogr. Inf. and Anal., Santa Barbara, Calif. ([http://www.ncgia.ucsb.edu/globalgrids-book/ease\\_grid/](http://www.ncgia.ucsb.edu/globalgrids-book/ease_grid/))
- Brown, J., and C. Haggerty (1998), Permafrost digital databases now available, *Eos Trans. AGU*, *79*(52), 634.
- Cao, Z., M. Wang, B. Proctor, G. Strong, R. Stewart, H. Ritchie, and J. Burnford (2002), On the physical processes associated with the water budget and discharge of the Mackenzie basin during the 1994/95 water year, *Atmos. Ocean*, *40*(2), 125–143.
- Chang, A. T. C. (1997), Snow parameters derived from microwave measurements during the BOREAS winter field campaign, *J. Geophys. Res.*, *102*(D24), 29,663–29,671.
- Chang, A. T. C., J. L. Foster, and D. K. Hall (1987), Nimbus 7 SMMR derived global snow cover parameters, *Ann. Glaciol.*, *9*, 39–44.
- Clark, M. P., M. C. Serreze, and D. A. Robinson (1997), Atmospheric controls on Eurasian snow extent, *Int. J. Climatol.*, *19*(1), 27–40.
- Derksen, C., E. LeDrew, and B. Goodison (2000), Temporal and spatial variability of North American prairie snow cover (1988–1995) inferred from passive microwave-derived snow water equivalent imagery, *Water Resour. Res.*, *36*(1), 255–266.
- Frei, A., and D. A. Robinson (1998), Evaluation of snow extent and its variability in the atmospheric model intercomparison project, *J. Geophys. Res.*, *103*(D8), 8859–8871.
- Frei, A., and D. A. Robinson (1999), Northern Hemisphere snow extent: Regional variability 1972–1994, *Int. J. Climatol.*, *19*(14), 1535–1560.
- Grabs, W. E., F. Fortmann, and De T. De Couel (2000), Discharge observation networks in Arctic regions: Computation of the river runoff into the Arctic Ocean, its seasonality and variability, in *The Freshwater Budget of the Arctic Ocean, Proceedings of the NATO Advanced Research Workshop, Tallin, Estonia, 27 April–1 May, 1998*, pp. 249–268, Springer, New York.
- Hulme, M. (1991), An intercomparison of model and observed global precipitation climatologies, *Geophys. Res. Lett.*, *18*, 1715–1718.
- Jones, P. D. (1994), Hemispheric surface air temperature variations: A reanalysis and an update to 1993, *J. Clim.*, *7*, 1794–1802.
- Kane, D. L. (1997), The impact of Arctic hydrologic perturbations on Arctic ecosystems induced by climate change, in *Global Change and Arctic Terrestrial Ecosystems, Ecol. Stud.*, vol. 124, pp. 63–81, Springer, New York.
- Kane, D. L., L. D. Hinzman, J. P. McNamara, Z. Zhang, and C. S. Benson (2000), An overview of a nested watershed study in Arctic Alaska, *Nord. Hydrol.*, *31*, 245–266.
- Lammers, R., A. Shiklomanov, C. Vorosmarty, B. Fekete, and B. Peterson (2001), Assessment of contemporary arctic river runoff based on observational discharge records, *J. Geophys. Res.*, *106*(D4), 3321–3334.
- Liston, G. E., and M. Sturm (1998), A snow-transport model for complex terrain, *J. Glaciol.*, *44*, 498–516.
- Liston, G. E., and M. Sturm (2002), Winter precipitation patterns in Arctic Alaska determined from a blowing-snow model and snow-depth observations, *J. Hydrometeorol.*, *3*, 646–659.
- Liston, G. E., and M. Sturm (2004), The role of winter sublimation in the Arctic moisture budget, *Nord. Hydrol.*, *35*(4), 325–334.
- Massom, R. (1995), Satellite remote sensing of polar now and ice: Present status and future directions, *Polar Rec.*, *31*(177), 99–114.
- Oelke, C., T. Zhang, M. C. Serreze, and R. L. Armstrong (2003), Regional-scale modeling of soil freeze/thaw over the Arctic drainage basin, *J. Geophys. Res.*, *108*(D10), 4314, doi:10.1029/2002JD002722.
- Pomeroy, J. W., D. W. Gray, and P. G. Landine (1993), The prairie blowing snow model: Characteristics, validation, operation, *J. Hydrol.*, *144*, 165–192.
- Proshutinsky, A., I. Polyakov, and M. Johnson (1999), Climate states and variability of Arctic ice and water dynamics during 1946–1997, *Polar Res.*, *18*(2), 135–142.
- Prowse, T. D., and P. O. Flegg (2000), Arctic river flow: A review of contributing areas, in *The Freshwater Budget of the Arctic Ocean, Proceedings of the NATO Advanced Research Workshop, Tallin, Estonia, 27 April–1 May 1998*, pp. 269–280, Springer, New York.
- Rango, A. (1996), Spaceborne remote sensing for snow hydrology applications, *Hydrol. Sci. J.*, *41*(4), 477–494.
- Rango, A. (1997), Response of areal snow cover to climate change in a snowmelt-runoff model, *Ann. Glaciol.*, *25*, 232–236.
- Rango, A., and A. I. Shalaby (1999), Current operational applications of remote sensing in hydrology, *Oper. Hydrol. Rep.* *43*, 73 pp., World Meteorol. Organ., Geneva, Switzerland.
- Robinson, D. A., and A. Frei (2000), Seasonal variability of Northern Hemisphere snow extent using visible satellite data, *Prof. Geogr.*, *52*(2), 307–314.
- Robinson, D. A., K. F. Dewey, and R. R. Heim Jr. (1993), Global snow cover monitoring: An update, *Bull. Am. Meteorol. Soc.*, *74*, 1689–1696.
- Semiletov, I. P., N. I. Savelieva, G. E. Weller, I. I. Popko, S. P. Pugach, Y. Gukov, and L. N. Vasilevskaya (2000), The dispersion of Siberian river flows into coastal waters: Meteorological, hydrological and hydrochemical aspects, in *The Freshwater Budget of the Arctic Ocean, Proceedings of the NATO Advanced Research Workshop, Tallin, Estonia, 27 April–1 May 1998*, pp. 323–366, Springer, New York.
- Serreze, M. C., J. A. Maslanik, G. Scharfen, and R. G. Barry (1993), Interannual variations in snow melt over Arctic sea ice and relationships to atmospheric forcings, *Ann. Glaciol.*, *17*, 327–331.
- Serreze, M. C., J. E. Walsh, E. C. Chapin, T. Osterkamp, M. Dyugero, V. Romanovsky, W. C. Oechel, J. Morison, T. Zhang, and R. G. Barry (2000), Observation evidence of recent change in the northern high-latitude environment, *Clim. Change*, *46*, 159–207.
- Serreze, M. C., D. H. Bromwich, M. P. Clark, A. J. Etringer, T. Zhang, and R. B. Lammers (2002), The large scale-hydro-climatology of the terrestrial arctic drainage system, *J. Geophys. Res.*, *107*, 8160, doi:10.1029/2001JD000919, [printed 108 (D2), 2003].
- Shiklomanov, I. A., A. I. Shiklomanov, R. B. Lammers, B. J. Peterson, and C. J. Vorosmarty (2000), The dynamics of river water inflow to the Arctic Ocean, in *The Freshwater Budget of the Arctic Ocean, Proceedings of the NATO Advanced Research Workshop, Tallin, Estonia, 27 April–1 May 1998*, pp. 281–296, Springer, New York.
- Skaugen, T. (1999), Estimating the mean areal snow water equivalent by integration in time and space, *Hydrol. Processes*, *13*(12/13), 2051–2066.
- Steffen, K., R. Bindshadler, G. Casassa, J. Comiso, and D. Eppler (1993), Snow and ice applications of AVHRR in polar regions: 3rd Symposium on Remote Sensing of Snow and Ice, Boulder, CO, May 17–22, 1992, *NASA Tech. Memo.*, *NASA-TM-113076*, 16 pp.
- Vörösmary, C. J., L. D. Hinzman, B. J. Peterson, D. H. Bromwich, L. C. Hamilton, J. Morison, V. E. Romanovsky, M. Sturm, and R. S. Webb (2001), the hydrologic cycle and its role in Arctic and global environmental change: A rationale and strategy for synthesis study, 84 pp., Arct. Res. Consortium of the U.S., Fairbanks, Alaska.
- Walker, A. E., and B. E. Goodison (1993), Discrimination of a wet snow cover using passive microwave satellite data, *Ann. Glaciol.*, *17*, 307–311.
- Walker, A. E., and A. Silis (2002), Snow-cover variations over the Mackenzie River basin, Canada, derived from SSM/I passive-microwave satellite data, *Ann. Glaciol.*, *34*, 8–14.
- Walsh, J. E. (2000), Global atmospheric circulation patterns and relationships to Arctic freshwater fluxes, in *The Freshwater Budget of the Arctic Ocean, Proceedings of the NATO Advanced Research Workshop, Tallin, Estonia, 27 April–1 May 1998*, pp. 21–41, Springer, New York.
- Whitfield, P., and A. Cannon (2000), Recent climate moderated shifts in Yukon hydrology, in paper presented at Water Resources in Extreme Environments, Am. Water Resour. Assoc., Anchorage, Alaska, 1–3 May.
- Woo, M.-K. (1986), Permafrost hydrology in North America, *Atmos. Ocean*, *24*(3), 201–234.
- Yang, D., and T. Ohata (2001), A bias corrected Siberian regional precipitation climatology, *J. Hydrometeorol.*, *2*(1), 122–139.
- Yang, D., D. Kane, L. Hinzman, X. Zhang, T. Zhang, and H. Ye (2002), Siberian Lena River hydrologic regime and recent change, *J. Geophys. Res.*, *107*(D23), 4694, doi:10.1029/2002JD002542.
- Yang, D., D. Robinson, Y. Zhao, T. Estilow, and B. Ye (2003), Streamflow response to seasonal snow cover extent changes in large Siberian watersheds, *J. Geophys. Res.*, *108*(D18), 4578, doi:10.1029/2002JD003149.

- Yang, D., B. Ye, and A. Shiklomanov (2004a), Streamflow characteristics and changes over the Ob river watershed in Siberia, *J. Hydrometeorol.*, 5(4), 595–610.
- Yang, D., B. Ye, and D. Kane (2004b), Streamflow changes over Siberian Yenisei river basin, *J. Hydrol.*, 296, 59–80.
- Yang, D., D. Kane, Z. Zhang, D. Legates, and B. Goodison (2005), Bias-corrections of long-term (1973–2004) daily precipitation data over the northern regions, *Geophys. Res. Lett.*, 32, L19501, doi:10.1029/2005GL024057.
- Yang, Z. L., R. E. Dickinson, A. N. Hahmann, G.-Y. Niu, M. Shaikh, X. Gao, R. C. Bales, S. Sorooshian, and J. Jin (1999), Simulation of snow mass and extent in general circulation models, *Hydrol. Processes*, 13(12/13), 2097–2113.
- Ye, B., D. Yang, and D. Kane (2003), Changes in Lena River streamflow hydrology: Human impacts vs. natural variations, *Water Resour. Res.*, 39(8), 1200, doi:10.1029/2003WR001991.
- Ye, H., H. Cho, and P. E. Gustafson (1998), The changes in Russian winter snow accumulation during 1936–83 and its spatial patterns, *J. Clim.*, 11, 856–863.
- Zhang, T. (2005), Influence of the seasonal snow cover on the ground thermal regime: An overview, *Rev. Geophys.*, 43, RG4002, doi:10.1029/2004RG000157.
- Zhang, T., R. G. Barry, K. Knowles, J. A. Heginbottom, and J. Brown (1999), Statistics and characteristics of permafrost and ground-ice distribution in the Northern Hemisphere, *Polar Geogr.*, 23(2), 132–154.
- Zhang, X., K. D. Harvey, W. D. Hogg, and T. R. Yuzyk (2001), Trends in Canadian streamflow, *Water Resour. Res.*, 37, 987–998.
- 
- R. Armstrong and M.-J. Brodzik, National Snow and Ice Data Center, University of Colorado, Boulder, CO 80309-0449, USA.
- D. Robinson, Department of Geography, Rutgers University–State University of New Jersey, Piscataway, NJ 08854-8054, USA.
- D. Yang and Y. Zhao, Water and Environmental Research Center, 457 Duckering Building, University of Alaska Fairbanks, Fairbanks, AK 99775-5860, USA. (ffdy@uaf.edu)